



SCATTERING FROM SURFACES WITH DIFFERENT  
ROUGHNESS SCALES; ANALYSIS AND INTREPRETATION

William H. Peake and Donald E. Barrick

The Ohio State University

**ElectroScience Laboratory**

(formerly Antenna Laboratory)

Department of Electrical Engineering  
Columbus, Ohio 43212

TECHNICAL REPORT 1388-26

15 September 1967

Grant Number NsG-213-61

National Aeronautics and Space Administration  
Office of Grants and Research Contracts  
Washington, D.C. 20546

FACILITY FORM 602

N67-39091

(ACCESSION NUMBER)	(THRU)
68	
(PAGES)	(CODE)
1	07
(NASA CR OR TMX OR AD NUMBER)	
C1-81320	
(CATEGORY)	

## NOTICES

When Government drawings, specifications, or other data are used for any purpose other than in connection with a definitely related Government procurement operation, the United States Government thereby incurs no responsibility nor any obligation whatsoever, and the fact that the Government may have formulated, furnished, or in any way supplied the said drawings, specifications, or other data, is not to be regarded by implication or otherwise as in any manner licensing the holder or any other person or corporation, or conveying any rights or permission to manufacture, use, or sell any patented invention that may in any way be related thereto.

The Government has the right to reproduce, use, and distribute this report for governmental purposes in accordance with the contract under which the report was produced. To protect the proprietary interests of the contractor and to avoid jeopardy of its obligations to the Government, the report may not be released for non-governmental use such as might constitute general publication without the express prior consent of The Ohio State University Research Foundation.

## REPORT

by

The Ohio State University ElectroScience Laboratory  
(Formerly Antenna Laboratory)  
Columbus, Ohio 43212

Sponsor	National Aeronautics and Space Administration Office of Grants and Research Contracts Washington, D.C. 20546
Grant Number	NsG-213-61
Investigation of	Theoretical and Experimental Analysis of the Electromagnetic Scattering and Radiative Properties of Terrain, with Emphasis on Lunar-Like Surfaces
Subject of Report	Scattering from Surfaces with Different Roughness Scales; Analysis and Interpretation
Submitted by	William H. Peake and Donald E. Barrick ElectroScience Laboratory The Ohio State University Department of Electrical Engineering
Date	15 September 1967

## ABSTRACT

This paper discusses several approaches to scattering from slightly rough, very rough, composite, and rough spherical surfaces.

Average incoherent scattering cross sections for slightly rough surfaces are obtained using a perturbation technique for a perfect conductor, and for a surface material which is homogeneous (with variable permeability,  $\mu_r$ , as well as permittivity,  $\epsilon_r$ ). The results, correct to the first order, include polarization dependence, and particular solutions with curves are presented for the vertical, horizontal, and circular states. They are compared with measured data. The scattering process for this class of surfaces is interpreted physically.

Three optics techniques yielding results for very rough surface scattering cross sections are presented, and it is shown that they all give the same solution for Gaussian surfaces. Both homogeneous and perfectly conducting surface materials are treated, and polarization dependence is preserved. The restrictions under which the solutions are valid are enumerated. The physical interpretations of the scattering mechanism for this class of surfaces are discussed and shed valuable insight on the process. Curves are shown for backscattering, employing two probability models.

Surfaces consisting of both very rough and slightly rough structures together, termed composite surfaces, are analyzed, and an heuristic physical derivation of their scattering cross section is presented. Curves for backscattering cross section are shown, and comparison with measured results confirms the validity of this approach.

Average backscattering cross sections for rough spherical surfaces are presented. Both the coherent and incoherent cross sections are given for slightly and very rough spheres. These results have application to planetary surface radar scatter and to passive satellite communications.

The large volume of published material on the subject is reviewed. The first two parts dealing with slightly rough and very rough surfaces, rather than retrace detailed mathematical derivations available elsewhere, attempt to accomplish five goals: (i) to compare the various analyses already available, (ii) to elucidate explicitly the approximations involved in each approach, (iii) to explain and interpret the physical process behind the mathematics producing the scattering, (iv) to present meaningful

closed form mathematical solutions and curves, many of which have not appeared before, for the scattering cross sections, and (v) to compare theory with measurements. The material in the last two sections, treating composite and rough spherical surfaces, is new as far as the Western literature is concerned, and is based directly on the results of the first two sections; physical interpretation of the scattering mechanism again is emphasized.

## TABLE OF CONTENTS

	<u>Page</u>
I. INTRODUCTION	1
II. SLIGHTLY ROUGH PLANAR SURFACE	3
A. <u>Introduction</u>	3
B. <u>Analysis</u>	6
C. <u>Results for Vertical and Horizontal Polarization States</u>	16
1. <u>Bistatic scattering matrix elements for homogeneous surface</u>	17
2. <u>Backscattering matrix elements for homogeneous surface</u>	17
3. <u>Bistatic scattering matrix elements for perfectly conducting surface</u>	18
4. <u>Backscattering matrix elements for perfectly conducting surface</u>	18
D. <u>Results for Circular Polarization States</u>	21
1. <u>Bistatic scattering matrix elements</u>	21
2. <u>Backscattering matrix elements</u>	22
E. <u>Results for Arbitrary Linear Polarization States</u>	24
1. <u>Backscattering with aligned and crossed linear polarized antenna</u>	24
2. <u>Angularly averaged backscattering with aligned and crossed linear polarized antennas</u>	25
F. <u>Comparison with Measured Results</u>	25
III. VERY ROUGH PLANAR SURFACE	26
A. <u>Introduction</u>	26
B. <u>Review and Interpretation</u>	29
1. <u>Physical optics approach</u>	29
2. <u>Ray optics approach</u>	32
3. <u>Geometrical optics or stationary phase approach</u>	35

TABLE OF CONTENTS (cont.)

	Page
C. <u>Results</u>	37
1. <u>General form</u>	37
a. <u>Gaussian surface height</u>	
<u>joint probability density</u>	38
b. <u>Exponential surface height</u>	
<u>joint probability density</u>	39
2. <u>Polarization dependence</u>	39
a. <u>Vertical and horizontal states</u>	39
b. <u>Circular states and arbitrary</u>	
<u>polarized linear states</u>	40
3. <u>Results for backscattering</u>	40
a. <u>Gaussian surface height probability</u>	
<u>function model</u>	42
b. <u>Exponential surface height</u>	
<u>probability function model</u>	42
IV. COMPOSITE SURFACES	42
A. <u>Explanation</u>	42
V. ROUGH SPHERICAL SURFACE-	
BACKSCATTERING CROSS SECTION	50
A. <u>Introduction</u>	50
B. <u>Coherent Backscattering Cross Section</u>	52
C. <u>Average Incoherent Backscattering Cross</u>	
<u>Section - Slightly Rough Surface</u>	52
D. <u>Average Incoherent Backscattering Cross</u>	
<u>Section - Very Rough Surface</u>	56
E. <u>Average Incoherent Backscattering Cross</u>	
<u>Section - Composite Surface</u>	57
VI. SUMMARY	58
REFERENCES	60

## SCATTERING FROM SURFACES WITH DIFFERENT ROUGHNESS SCALES; ANALYSIS AND INTERPRETATION

### I. INTRODUCTION

Serious attempts to analyze the scattering of electromagnetic waves by rough surfaces and interfaces did not begin until about 1950. Research on this subject was stimulated to a large extent by an accumulation of measured data on radar scattering from terrain and the sea which was made during and immediately after World War II. Another stimulating factor was the significant expansion and dissemination of knowledge in the area of applied statistics which took place in the decade before 1950.

Since then, analysis of rough surface scattering has made use of one of two classes of surface model. The first, which we shall term the geometrical model, deals with surfaces made up of given deterministic shapes, but arranged or distributed in a random fashion; distributions of hemispherical bosses on a plane is an example of such a model analyzed by Twersky (1957). The second which we shall call the statistical model, treats the roughness height itself as a random variable from the outset. In the latter case, one must choose or specify the surface probability distributions or correlation coefficient. The statistical models seem more physically reasonable, since nature rarely composes a surface of given deterministic shapes. It is this second class of rough surface models which concerns us here. A review of the literature covering many of the rough surface scattering investigations is given in each respective section. More details, and results on other geometrical and statistical models can be found in Radar Cross Section Handbook (1968).

Statistically rough surfaces can be divided into three classes, distinguished by the relative roughness height compared to wavelength: slightly rough surfaces, intermediate, and very rough surfaces. The intermediate class has roughness features which lie in a region where neither high nor low frequency approximations apply. Only the slightly rough and very rough classes can be handled mathematically. In general, different techniques must be employed to solve these two classes. Much information can be obtained about the scattering behavior of rough surfaces from a study of these two classes, and it is not unreasonable to expect that extrapolation between them can give valuable insight into scatter from the intermediate class of rough surfaces.

Unfortunately, as with all new fields of investigation, errors and oversights have occurred. Soviet and Western developments in this area often paralleled each other; most investigators' articles and results went unnoticed by their foreign counterparts. Frequently, controversy in the literature over mistakes or minor details tended to obscure the positive and common points of agreement. Most serious of all, the emphasis on mathematical detail has in the majority of cases tended to obscure the simple physical concepts and processes producing the scattering. Also, many investigators were not careful in stating the approximations and assumptions inherent in their analyses; this has often led to misinterpretation and misuse by others.

We shall attempt here to emphasize the physical explanation of the scattering mechanism behind the mathematical formulations and solutions. Care is taken to outline the approximations and restrictions which apply to each model. Nonetheless results are presented in the most general form possible, including the effects of polarization and surface constitutive parameters. Several new results and explanations are offered for slightly rough surfaces, surfaces consisting of composite roughnesses of several scales, and rough spherical surfaces. In the case of very rough surfaces several existing analyses based upon different physical formulations are compared and shown to give identical results.

To introduce the terminology we shall use, imagine that a perfectly smooth surface becomes slightly rough. The average specularly reflected field present for the smooth surface decreases somewhat as the roughness grows; in addition there is a smaller amount of power scattered away from the specular direction due to the presence of the roughness. The former we shall call the coherent component while the latter is termed the incoherent component of the scattered field. More precisely, if one surface of an ensemble is replaced by another statistically similar member, or if the surface is translating slowly with respect to transmitter and receiver, the coherent component is distinguished by the fact that the average value of the complex field (existing at and near the specular direction) is non-zero. The incoherent field fluctuates, however; its phase angle is uniformly distributed; its average value is zero. On the other hand, the average scattered incoherent power (or incoherent field magnitude squared) is non-zero. As the roughness size increases, the coherent component decreases and the incoherent component increases. In the very rough surface limit, all of the scattered power is incoherent although it may be sharply beamed in the specular direction. This paper

is concerned mainly with the incoherent scattered power, except for the brief discussion below.

The coherent field scattered from a slightly rough surface is computed in the same fashion as it is for a smooth surface. In contrast to the incoherent component, it is highly dependent upon the shape of the illuminated area. It exhibits the familiar lobed structure of a flat plate, for example, while the incoherent component does not. Being concentrated around the specular direction, it can often be ignored in other directions. Experimentally, one can isolate the component by averaging first and then squaring the received voltage. The specular reflection coefficients for the slightly rough surface may be written in terms of the Fresnel coefficients for a smooth surface and a factor which accounts for roughness.

This modification is discussed in Radar Cross Section Handbook (1968) and can be determined for a Gaussian surface height. The resulting electric field reflection coefficients for that case are

$$(1) \quad R_{\parallel}^R(\theta_i) = R_{\parallel}(\theta_i) e^{-2k_o^2 h^2 \cos^2 \theta_i}, \quad R_{\perp}^R(\theta_i) = R_{\perp}(\theta_i) e^{-4k_o^2 h^2 \cos^2 \theta_i},$$

where  $R_{\parallel}(\theta_i)$  and  $R_{\perp}(\theta_i)$  are the usual Fresnel reflection coefficients for the smooth surface and are given in Eq. (35). The quantity  $\theta_i$  is the angle of incidence from normal,  $k_o = 2\pi/\lambda$  is the wave number, and  $h$  is the rms roughness height. As can be seen from the above, the effect of roughness on the coherent scattered field is contained in the exponential factor. It is this factor which quantitatively expresses the well-known Rayleigh criterion. Clearly, for  $k_o h < 1/4$ , the coherent component will be not significantly different from that of a smooth surface, and we call the surface "slightly rough". On the other hand if  $k_o h \cos \theta_i > 1$ , the coherent component will be insignificant, and we call the surface "very rough". The coherent component disappears as the roughness height,  $h$ , increases.

## II. SLIGHTLY ROUGH PLANAR SURFACE

### A. Introduction

In this section we will discuss an important class of random rough surfaces: those having a small scale of roughness whose rms roughness height,  $h$ , is much less than wavelength. In particular we shall obtain expressions for the incoherent average scattering cross sections per unit surface area,  $\sigma^0$ , for various polarization combinations. As

mentioned in the introduction, this cross section accounts for most of the scattered energy everywhere except in the neighborhood of the specular direction. At and near this direction, the coherent component is strong and cannot be neglected.

Slightly rough surface models have been employed in the past based upon the tangent plane, or Kirchhoff approximation. The first such analysis was that of Davies (1954). It has been discussed also by other workers, and a readable treatment is found in Beckmann and Spizzichino (1963 Section 5.3). It should be mentioned, however, that those models are often inapplicable to natural surfaces. The reason is that the tangent plane approximation restricts one to surfaces having  $2\pi\rho/\lambda \gg 1$ , where  $\rho$  is the local radius of curvature of the surface at all points. This requirement, along with the defining requirement  $2\pi h/\lambda \ll 1$  generally describes a very smooth, undulating surface with hills much less than wavelength in height and hundreds of wavelengths apart; the maximum slopes of these hills are infinitesimal. What is more, the model fails in the low frequency limit, since wavelength eventually becomes larger than surface radii of curvature. Also, the model shows no polarization dependence for backscatter, as is typical of models based upon the tangent plane approximation. Experimental evidence shows that radar backscatter does depend upon polarization; this will be discussed again later.

For the above reasons, we shall avoid use of the Kirchhoff approximation for the slightly rough surface model. Instead, we will resort to a much less restrictive model, but interestingly enough, a model originally formulated before that of Davies by Rice (1951). Rice's formulation was later developed by Peake (1959) who derived the scattering cross-sections. This model is based on a perturbation approach. Since the tangent plane assumption is not employed, all of the accompanying approximations such as neglect of multiple scattering and shadowing are avoided. The model is therefore valid for grazing incidence and scattering angles, and exhibits meaningful polarization dependence. Most important, it is valid in the low frequency limit and can apply to any of the class of very rough surfaces to be examined later when the frequency is low enough.

Valenzuela (1967) recently extended the same technique to obtain expressions for the second order perturbation correction terms for backscatter from dielectric and perfectly conducting surface. Only the first order terms of the solution are obtained here.

The following are the restrictions on the class of surfaces to which the model applies:

(a)  $k_0 \zeta(x, y) < 1.0$ , i.e., roughness height is small compared to wavelength,  $\lambda$ ;  $\zeta(x, y)$  is the height of the rough surface above the x-y plane, which is taken to be the mean surface plane.

(b)  $\partial \zeta / \partial x, \partial \zeta / \partial y < 1.0$ , i.e., surface slopes are relatively small.

(c)  $\langle \partial \zeta / \partial x^2 \rangle = \langle \partial \zeta / \partial y^2 \rangle$ , i.e., the roughness is isotropic. Here, the brackets  $\langle \rangle$  indicate average over an ensemble of surfaces. This restriction is not essential to the solution, but is employed here for simplicity.

(d)  $L \gg \ell, \lambda$ , i.e., the dimension,  $L$ , of the illuminated area is much greater than either the roughness correlation length,  $\ell$ , or the wavelength.\*

Since the tangent plane approximation is not employed, the mutual interaction effects of shadowing and multiple scattering are not overlooked. Hence the slightly rough surface solution includes these mechanisms. In fact, mutual interaction between neighboring hills is an important contributor when the distance between them is less than a wavelength.

We shall obtain first results for the average incoherent scattering cross section per unit surface area for a surface of homogeneous material having relative permeability,  $\mu_r$ , and permittivity,  $\epsilon_r$ . In this respect our results differ from the analysis of Rice (1951), Peake (1959), and Valenzuela (1967), who treat only dielectric surfaces. The quantities  $\mu_r$  and  $\epsilon_r$  may be real or complex, representing a lossless or lossy material. Their magnitudes may be greater, equal to, or less than unity, so that the important class of plasma media can be included. As a special case, the imaginary part of  $\epsilon_r$  can approach infinity, yielding the proper results for a perfectly conducting surface. The notation of Rice (1951), Peake (1959), and Valenzuela (1967), will

---

\* Also implied in the definition of scattering cross section is the restriction that the observation point must be in the far field of the surface. In the absence of roughness, this requirement means that the distance to the observation point,  $R$ , must satisfy the criterion  $R > 2L^2/\lambda$ . However, it can be shown (see Barrick, 1965) that when one is considering the incoherent scattered power from a roughened surface, this requirement reduces to  $R > 2\ell^2/\lambda$ , where  $\ell$  is the roughness correlation length. Physically this means that one can be considerably closer to a rough surface than a smooth one, since  $\ell \ll L$  by (d) above.

be employed as much as possible here, so that readers wishing a more detailed derivation can refer to that work. The solution for a horizontally polarized incident plane wave will be obtained here. Similar results for vertical incident polarization will be then written from inspection by interchanging the roles of  $E$  and  $H$ ,  $\epsilon_r$  and  $\mu_r$ . From these results, the pertinent values for the circular polarization states and for linear polarization states of arbitrary orientation will be given.

### B. Analysis

The time convention used here will be  $e^{-i\omega t}$ . The analyses of Rice, Peake, and Valenzuela are compatible with this if one replaces  $i$  there by  $-i$ , since they use the positive time convention. Let us first consider one particular rough surface from an ensemble of statistically similar rough surfaces. For convenience, assume the surface to be square, of length  $L$ , centered about the origin and with its mean surface coinciding with the  $x$ - $y$  plane (Fig. 1). Later in the analysis, the surface length will be permitted to approach infinity; the square shape

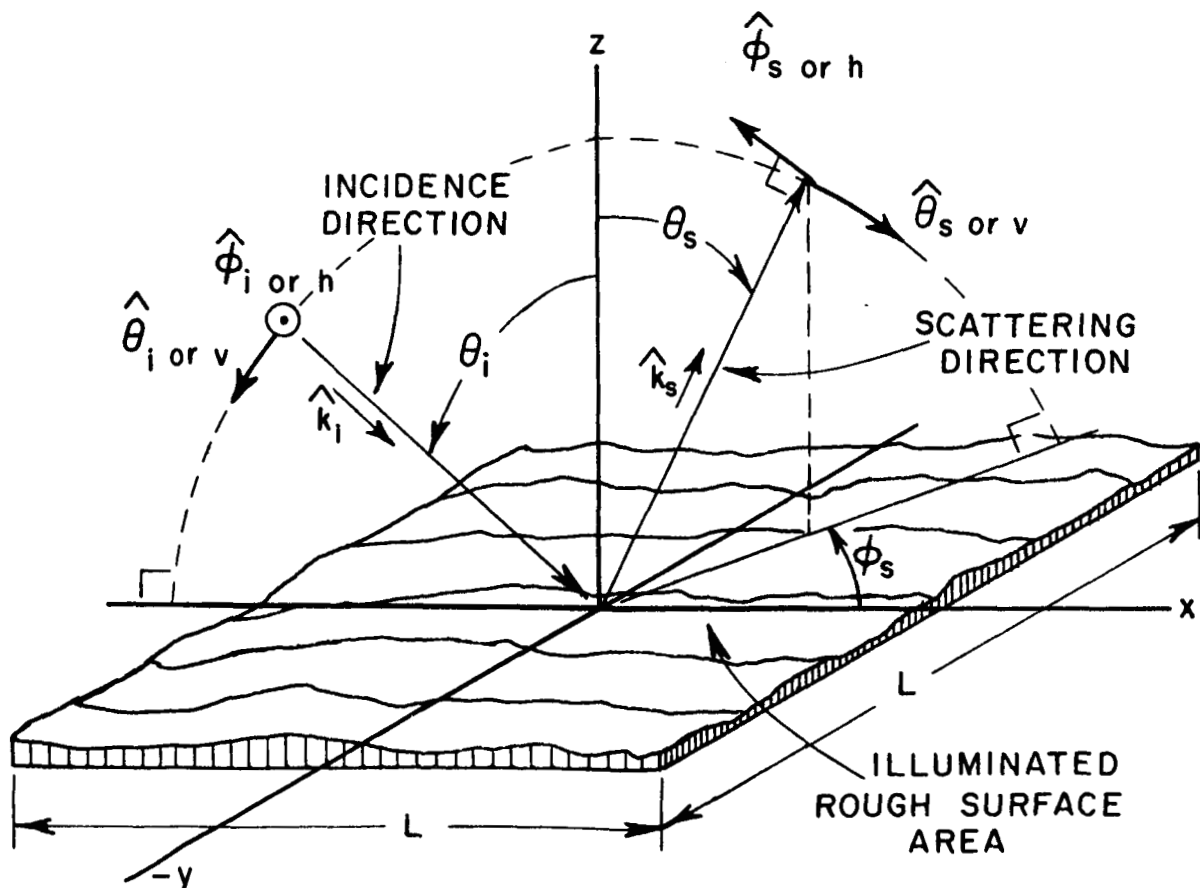


Fig. 1. Surface arrangement and scattering geometry.

of the surface is irrelevant to the results, but is a useful artifice in performing the derivation. Under these conditions, the surface height can be expanded in the following Fourier series:

$$(2) \quad \zeta(x, y) = \sum_{m, n=-\infty}^{\infty} P(m, n) e^{ia(mx+ny)},$$

$$\text{where } a = \frac{2\pi}{L}.$$

The real nature of the surface height requires that  $P(-m, -n) = P^*(m, n)$  where the asterisk denotes complex conjugate. The trick in simplifying the analysis is to expand the scattered, or perturbed, field into a Fourier series with eigenfunctions  $e^{ia(mx+ny)}$ . Physically this means representing these fields as a superposition of plane waves in all directions. Remembering that the incident field is horizontally polarized in the  $y$ -direction as shown in Fig. 1, the total  $E$ -field in free space above the surface is then written as follows:

$$(3a) \quad E_x^+ = E_x^s$$

$$(3b) \quad E_y^+ = E^i + E^r + E_y^s,$$

$$(3c) \quad E_z^+ = E_z^s,$$

where  $E^i$  is the incident field, and  $E^r$  is the reflected field from a perfectly smooth homogeneous surface. The terms with the superscript,  $s$ , are then due solely to the presence of roughness, and may be considered the incoherent scattered or perturbed fields. These quantities are given as

$$(4a) \quad E^i = E_y^0 e^{-\sigma\alpha x + \sigma\gamma z}; \quad E^r = R E_y^0 e^{-\sigma\alpha x - \sigma\gamma z},$$

$$(4b) \quad E_x^s = \sum_{m, n=-\infty}^{\infty} A_{mn} e^{ia(mx+ny)} \cdot e^{ib(m, n)z},$$

$$(4c) \quad E_y^s = \sum_{m,n=-\infty}^{\infty} B_{mn} e^{ia(mx+ny)} \cdot e^{ib(m,n)z},$$

$$(4d) \quad E_z^s = \sum_{m,n=-\infty}^{\infty} C_{mn} e^{ia(mx+ny)} \cdot e^{ib(m,n)z}.$$

In these equations,  $\sigma = -ik_o = i\omega\sqrt{\epsilon_0\mu_0}$ ,  $\alpha = \sin \theta_i$ ,  $\gamma = \cos \theta_i$ , and  $E_y^0$  is the electric field strength of the incident field.  $R$  is the Fresnel reflection coefficient for horizontal polarization, and is given by

$$(4e) \quad R = \frac{1 - \frac{\tau \gamma'}{\mu_r \sigma \gamma}}{1 + \frac{\tau \gamma'}{\mu_r \sigma \gamma}}, \text{ where } \tau = ik_o \sqrt{\epsilon_r \mu_r} \text{ and } \gamma' = \frac{1}{\sqrt{\epsilon_r \mu_r}} \sqrt{\epsilon_r \mu_r - \alpha^2}$$

The function  $b(m, n)$  is not independent of the wavenumbers in the  $x$  and  $y$  direction, and is dictated by the requirement that each term of the above series must satisfy the wave equation. This results in the following relationship:

$$(5) \quad b(m, n) = \sqrt{k_o^2 - a^2 (m^2 + n^2)} = i\sqrt{\sigma^2 + a^2 (m^2 + n^2)}.$$

The objective is to derive  $A_{mn}$ ,  $B_{mn}$ , and  $C_{mn}$  in terms of  $P(m, n)$  and all of the above parameters. This is done by a standard perturbation technique and the details are similar to those of Rice, Peake, and Valenzuela. Briefly, these three coefficients are obtained by expanding all quantities possible into series, each term of which involves a higher power of the smallness parameters, which are taken to be  $k_o \zeta$ ,  $\partial \zeta / \partial x$ , and  $\partial \zeta / \partial y$ . By assumptions (a) and (b), these quantities are small, and consequently only the first term of these series need be retained. The above three unknown coefficients (as well as three other unknown coefficients,  $G_{mn}$ ,  $H_{mn}$ ,  $I_{mn}$  which represent the scattered fields inside the surface material) are obtained from six equations, four of which come from the boundary conditions for the  $E$  and  $H$  fields at the interface  $z = \zeta$ , and two of which arise from the divergence conditions on each side of the interface.

The three desired coefficients  $A_{mn}$ ,  $B_{mn}$ , and  $C_{mn}$  are then correct to the first order, i.e., the neglected terms are at least of order  $k_0 \zeta$ ,  $\partial \zeta / \partial x$ , or  $\partial \zeta / \partial y$  with respect to the result shown. The terms of the next higher order are derived by Rice (1951) and Valenzuela (1967) for perfectly conducting and dielectric surfaces, but they are not given here. Also it should be noted that each of these coefficients is directly proportional to  $P(m-v, n)$ , the  $m-v$ ,  $n$ -th coefficient in the Fourier expansion for the surface itself. ( $v \equiv k_0 \sin \theta_i / a$ , and is taken to be an integer here, i.e., the possible directions of incidence are quantized for the moment. However, in the limit as  $a = 2\pi/L \rightarrow 0$  with  $L \rightarrow \infty$ ,  $v$  becomes large, and thus it is possible to approximate it by the nearest integer with negligible error.)

Up to now, no restrictions have been placed on the nature of the surface. The surface may in fact be deterministic or periodic. For example in the case of a one-dimensional sinusoidal surface of period  $L$ , the expansion for the surface,  $\zeta(x)$ , degenerates to the situation where  $P(j, k) \equiv 0$  for  $j \neq \pm 1$  and  $k \neq 0$ ; this important case was solved long ago by Lord Rayleigh (Dover, 1945). To gain insight into the scattering process for the slightly rough surface, it is instructive to point out a fact about this surface. The vanishing of all but two of the coefficients  $P(m-v, n)$  means that the coefficients for the scattered field expansions of Eqs. (3b), (3e), i.e.,  $A_{mn}$ ,  $B_{mn}$ , and  $C_{mn}$ , all vanish except when  $n = 0$  and  $m = v \pm 1$ . In other words, the scattered field consists of only two plane waves, propagating in two directions determined by the direction of incidence and the wavelength-to-surface period. These waves are both in the plane of incidence (i.e.,  $x-z$  plane), and the scattering angle is determined by the equation  $\sin \theta_s = \sin \theta_i \pm \lambda/L$ . It is important to note that these waves exist physically only when  $|\sin \theta_s| = |\sin \theta_i \pm \lambda/L| < 1$ ; when  $\lambda/L$  is such that this inequality is not satisfied, the propagation number,  $b(m, n)$  is pure imaginary, indicating an evanescent or non-radiating mode. For period much larger than wavelength, scattering takes place close to the specular direction. As  $\lambda/L$  becomes larger, the two scattered plane waves diverge from the specular direction until they reach grazing ( $|\sin \theta_s| = 1$ ), at which point the plane waves are cut off. Hence the scattering directions are determined not by the amplitude of the sinusoidal surface (so long as it satisfies the "slightly rough" criterion) but by its period compared to wavelength. This behavior is also exhibited by the random rough surface considered below.

Before discussing the scattering, let us discuss the parameters involved in the statistical description of the surface,  $\zeta(x, y)$ . Davenport and Root (1958) employ Rice's earlier work (1944, 1945) to show that

a random but periodic function of period  $L$  can be expanded in a Fourier series such as Eq. (2), where the coefficients  $P(m, n)$  are random variables. Going further, they show that these coefficients become uncorrelated in the limit as  $L \rightarrow \infty$ . Practically, it is necessary only that  $L > > l$ , i.e., the total surface length must be much greater than the roughness correlation length; this is exactly restriction (d) above. Now, recalling that the mean value of the surface is zero, these conditions become.

$$(6a) \quad \langle P(m, n) \rangle = 0$$

$$(6b) \quad \langle P(m, n) P(u, v) \rangle = \begin{cases} 0 & \text{for } u, v = m, n \\ \frac{\pi^2}{L^2} W(p, q) & \text{for } u, v = m, n \end{cases}$$

where  $p = am = 2\pi m/L$  and  $q = an = 2\pi n/L$ . The function  $W(p, q)$  is physically the roughness spectral density of the surface, and  $p, q$  are radian wave numbers. Using these equations, the following relationships are obtained.

$$(7a) \quad \begin{aligned} \langle \zeta^2(x, y) \rangle &= \sum_{m, n, u, v} \langle P(m, n) P(u, v) \rangle e^{i\alpha x(m-u) + i\alpha y(n-v)} \\ &= \sum_{m, n} \langle P(m, n) P(-m, -n) \rangle \rightarrow \int_{-\infty}^{\infty} dm \int_{-\infty}^{\infty} dn \frac{\pi^2}{L^2} W(p, q) \\ &= \frac{1}{4} \int_{-\infty}^{\infty} \int_{-\infty}^{\infty} W(p, q) dp dq \equiv h^2, \end{aligned}$$

$$(7b) \quad \begin{aligned} \langle \zeta(x, y) \zeta(x', y') \rangle &= \sum_{m, n, u, v} \langle P(m, n) P(u, v) \rangle e^{iamx + iaux' + iany + iavy'} \\ &= \sum_{m, n} \langle P(m, n) P(-m, -n) \rangle e^{iam(x-x') + ian(y-y')} \\ &\rightarrow \frac{1}{4} \int_{-\infty}^{\infty} \int_{-\infty}^{\infty} W(p, q) e^{ip\tau_x + iq\tau_y} dp dq \equiv h^2 R(\tau_x, \tau_y) \end{aligned}$$

where  $\tau_x = x - x'$ , and  $\tau_y = y - y'$ . The quantity  $h^2$ , as mentioned earlier, is the surface mean square height, and  $R(\tau_x, \tau_y)$  is the surface height correlation coefficient. Relationship (7b) merely states that the roughness height spectral density and the surface height correlation function are Fourier transforms.

Now, let us determine the horizontal (h) and vertical (v) components of the plane wave scattered field in a given direction represented by the angles  $\theta_s, \phi_s$ ; first it is necessary to relate the wave numbers  $a_m$  and  $a_n$  of the exponentials of Eqs. (4b)-(4d) to the propagation constant of the plane waves in spherical coordinates. This relationship is obvious:

$$(8) \quad a_m = k_0 \sin \theta_s \cos \phi_s, \text{ and } a_n = k_0 \sin \theta_s \sin \phi_s.$$

Then the horizontal and vertical components of the scattered plane wave in the direction corresponding to  $m, n$  are

$$(9) \quad E_h^s(m, n) = (-A_{mn} \sin \phi_s + B_{mn} \cos \phi_s) e^{ia(mx + ny) + ib(m, n)z},$$

and

$$(9b) \quad E_v^s(m, n) = (A_{mn} \cos \theta_s \cos \phi_s + B_{mn} \cos \theta_s \sin \phi_s - C_{mn} \sin \theta_s) e^{ia(mx + ny) + ib(m, n)z}.$$

Let us redefine these relationships in terms of quantities ( $\alpha_{hh}$  and  $\alpha_{vh}$ ) which are directly proportional to scattering matrix elements, namely

$$(10a) \quad E_h^s(m, n) = 2k_0 E_y^0 \alpha_{hh} \cos \theta_i P(m - v, n) e^{ia(mx + ny) + ib(m, n)z},$$

and

$$(10b) \quad E_v^s(m, n) = 2k_0 E_y^0 \alpha_{vh} \cos \theta_i P(m - v, n) e^{ia(mx + ny) + ib(m, n)z}.$$

The quantities  $\alpha_{hh}$  and  $\alpha_{vh}$  are determinable from Eqs. (9) and the expressions for  $A_{mn}$ ,  $B_{mn}$ ,  $C_{mn}$ . They will be given in simplified form subsequently, along with expressions for the other two elements  $\alpha_{hv}$  and

$\alpha_{vv}$  for vertical incident polarization. Note that the random nature of the rough surface is reflected explicitly in the surface coefficients above,  $P(m-\nu, n)$ . The factors  $\alpha_{hh}$  and  $\alpha_{vh}$  are nonrandom, known functions. At this point, the average scattering cross sections can be determined. First, let us find the increment in average field intensity in all of the plane waves between  $m_1$  and  $m_2$ ,  $n_1$  and  $n_2$ . For arbitrary polarizations,  $\gamma$ ,  $\delta$ , this is given by

$$(11) \quad \Delta \langle |E_Y^S(m, n)|^2 \rangle = 4k_0^2 |E_0^0|^2 \cos^2 \theta_i \sum_{m_1}^{m_2} \sum_{n_1}^{n_2} |\alpha_{Y\delta}|^2 \langle P(m-\nu, n) P^*(m-\nu, n) \rangle$$

where use is made of the orthogonal properties of the coefficients, as stated in Eq. (6b). If the length of the surface,  $L$ , is large compared to wavelength,  $\lambda$ , there are many such plane waves between  $m_1$  and  $m_2$  (as well as between  $n_1$  and  $n_2$ ). The terms in the summation are then nearly constant for  $m_1 < m < m_2$  (as well as  $n_1 < n < n_2$ ) for  $m_2$  sufficiently near  $m_1$ , and the summation can be rewritten

$$(12) \quad \Delta \langle |E_Y^S(m, n)|^2 \rangle = 4k_0^2 |E_0^0|^2 \cos^2 \theta_i |\alpha_{Y\delta}|^2 \langle P(m-\nu, n) P^*(m-\nu, n) \rangle (m_2 - m_1) (n_2 - n_1)$$

$$= 4k_0^2 \frac{\pi^2}{L^2} |E_0^0|^2 \cos^2 \theta_i |\alpha_{Y\delta}|^2 W(\Delta m - \Delta n, \Delta m \Delta n),$$

where  $\Delta m = m_2 - m_1$  and  $\Delta n = n_2 - n_1$ .

Using the above expression, the increment of intensity per unit of solid angle,  $\Omega_s$ , is expressed in terms of the Jacobian,  $\Delta m \Delta n / \Delta \Omega_s$ .

$$(13) \quad \frac{\Delta \langle |E_Y^S(\theta_s, \phi_s)|^2 \rangle}{\Delta \Omega_s} = \frac{4k_0 \pi^2}{L^2} |E_0^0|^2 \cos^2 \theta_i |\alpha_{Y\delta}|^2 W[k_0(\sin \theta_s \cos \phi_s - \sin \theta_i), k_0 \sin \theta_s \sin \phi_s] \frac{\Delta m \Delta n}{\Delta \Omega_s}$$

Noting that  $\Omega_s = \sin \theta_s d\theta_s d\phi_s$ , the Jacobian is

$$(14) \quad \frac{\Delta m \Delta n}{\Delta \Omega_s} = \frac{k_o^2 L^2}{4\pi^2} \cos \theta_s .$$

Hence the average field intensity at the receiver, or observation point, is the quantity in Eq. (13) multiplied by the solid angle subtended by the surface from the observation point. This is

$$\Delta \Omega_s = \frac{L^2 \cos \theta_s}{R^2} ,$$

so that

$$(15) \quad \langle |E_Y^s|^2 \rangle = \frac{\Delta \langle |E_Y^s(\theta_s, \phi_s)|^2 \rangle}{\Delta \Omega_s} = \frac{L^2 \cos \theta_s}{R^2} .$$

The average scattering cross section per unit surface area at the observation point and for incident, scattered polarization states  $\delta, \gamma$  is given by

$$\sigma_{\gamma\delta}^o(\theta_s, \phi_s) = \frac{\langle |E_Y^s|^2 \rangle 4\pi R^2}{L^2 |E_\delta^o|^2} ,$$

or

$$(16) \quad \sigma_{\gamma\delta}^o(\theta_s, \phi_s) = 4\pi k_o^4 \cos^2 \theta_i \cos^2 \theta_s |\alpha_{\gamma\delta}|^2 W[k_o(\sin \theta_s \cos \phi_s - \cos \theta_i), k_o \sin \theta_s \sin \phi_s] .$$

Restriction (c) assumed that the surface roughness is isotropic. This means that the height correlation function  $R(\tau_x, \tau_y)$  is a function only of the separation,  $r$ , between the surface points  $x, y$  and  $x', y'$ , (i.e.,  $r = \sqrt{(x-x')^2 + (y-y')^2} = \sqrt{\tau_x^2 + \tau_y^2}$ ). Hence, define

$$(17a) \quad \rho(r) = R(\tau_x, \tau_y) ,$$

applicable when the roughness is isotropic. This means that the roughness spectral density,  $W(p, q)$ , is also symmetrical in  $p$  and  $q$ . Define

$$t = \sqrt{p^2 + q^2} \text{ and}$$

$$(17b) \quad w(t) = W(p, q).$$

Then for an isotropic surface the Fourier transformation between the roughness spectral density and the correlation function, as given in Eq. (7b) reduces to the following Hankel transform pair.

$$(18a) \quad 4h^2 \rho(r) = 2\pi \int_0^\infty t w(t) J_0(rt) dt,$$

and

$$(18b) \quad w(t) = \frac{2h^2}{\pi} \int_0^\infty r \rho(r) J_0(rt) dr.$$

Then Eq. (16) may be rewritten

$$(19a) \quad \sigma_{Y\delta}^0(\theta_s, \phi_s) = \frac{4}{\pi} k_o^4 h^2 \cos^2 \theta_i \cos^2 \theta_s |\alpha_{Y\delta}|^2 \cdot I,$$

where

$$(19b) \quad I = \frac{\pi^2}{h^2} w(t) = 2\pi \int_0^\infty r \rho(r) J_0(rt) dr,$$

$$(19c) \quad t = k_o \sqrt{\sin^2 \theta_i - 2 \sin \theta_i \sin \theta_s \cos \phi_s + \sin^2 \theta_s}.$$

When the average incoherent scattering cross section per unit surface area is written as in Eq. (19a), the effect of the surface roughness is contained entirely in the factor  $h^2 I$ . The dependence upon incidence and scattering geometries, polarization states, and surface material properties is contained in the factors  $\cos^2 \theta_i \cos^2 \theta_s |\alpha_{Y\delta}|^2$ . As with all objects whose size is small compared to wavelength, the scattering cross section varies inversely as the fourth power of wavelength.

Let us now interpret Eqs. (19) physically. They indicate that the average intensity of the scattered field in a given direction varies in direct

proportion to the surface roughness spectral strength at surface roughness frequency,  $t$  (radians/meter). The quantity,  $t$ , in turn is a function of the incidence and scattering directions, as given in Eq. (19c). For example, for scattering near the specular direction,  $t \approx 0$ , the scattering cross section is directly proportional to the roughness spectral strength at and near DC. On the other hand, the highest roughness spectral frequencies which can affect the average incoherent scattered power are those at  $t = 2k_0$ . This occurs where  $\theta_i = \theta_s = \pi/2$  and  $\phi_s = \pi$ , i.e., for backscattering near grazing. Hence, the only possible surface roughness spectral frequencies which affect the average scattered power in any arbitrary direction occur in the range  $0 < t < 2k_0$ ; any higher roughness spectral frequencies present in the surface can have no effect on the scattered power, at least to the first order perturbation theory used here and subject to the restrictions listed above. The physical interpretation of the scattering process is similar to that for the sinusoidal surface mentioned previously.

Let us now examine two familiar choices for the surface roughness correlation coefficient,  $\rho(r)$ , and find the resulting spectral densities  $w(t)$  and the corresponding quantity  $I$ .

(1) Gaussian Surface Height Correlation Coefficient:  
 $\rho(r) = \exp(-r^2/\ell^2)$  .

Here,  $\ell$  is referred to as the surface height correlation length. The quantity  $I$  for this case becomes

$$(20) \quad I \approx \pi \ell^2 \exp(-t^2 \ell^2 / 4) \\ = \pi \ell^2 \exp[-(k_0^2 \ell^2 / 4) \times (\sin^2 \theta_i - 2 \sin \theta_i \sin \theta_s \cos \phi_s + \sin^2 \theta_s)] .$$

Surfaces having such a Gaussian surface height correlation coefficient are smoothly curving with derivatives at all points. The total mean square slope of the surface at any point with the above correlation coefficient is

$$(21) \quad s^2 = \left\langle \left( \frac{\partial \zeta}{\partial x} \right)^2 + \left( \frac{\partial \zeta}{\partial y} \right)^2 \right\rangle = \frac{4h^2}{\ell^2} .$$

(2) Exponential Surface Height Correlation Coefficient:  
 $\rho(r) = \exp(-|r|/\ell)$  .

The quantity  $I$  in this case becomes:

$$(22) \quad I = \frac{2\pi\ell^2}{[1 + t^2\ell^2]^{3/2}} = \frac{2\pi\ell^2}{[1 + k_0^2\ell^2(\sin^2\theta_i - 2\sin\theta_i\sin\theta_s + \sin^2\theta_s)]^{3/2}}$$

Surfaces with exponential correlation coefficients are jagged and have many vertical facets. The mean surface slopes and all higher surface derivatives are infinite, obviously because of these vertical facets. As an example, an urban area having buildings and houses comprising its scattering surface has a surface height correlation coefficient which behaves like the exponential, especially near the origin.

It should be noted that for  $2k_0\ell < 1$ , the behavior of  $I$  for the two correlation coefficients is not significantly different, except for a factor of 2. Nor are the above two correlation coefficient models necessarily the most applicable in all cases. Peake (1960) found that a model which empirically fitted measured points for the correlation coefficient of an asphalt surface was

$$\rho(r) = [1 + 20r^2]^{-3/2}$$

where  $r$  is in cm. By the Hankel transformation between  $I$  and  $\rho(r)$ , in this case  $I$  is an exponential function of  $t$ .

### C. Results for Vertical and Horizontal Polarization States

We obtained above the average incoherent scattering cross section for a horizontally polarized incident plane wave and for the horizontally and vertically polarized scattered components. We left them in terms of scattering matrix elements,  $\alpha_{hh}$  and  $\alpha_{vh}$ , which are determined by Eqs. (9) and (10). The resulting cross sections and scattering matrix elements,  $\alpha_{hv}$  and  $\alpha_{vv}$ , for a vertically polarized incident plane wave may be found immediately by noting that a vertically polarized plane wave (vertical or  $\theta$  directed E-field) is identical to a horizontally directed H-field vector. Hence the quantities  $\alpha_{hv}$  and  $\alpha_{vv}$  may be obtained from  $\alpha_{vh}$  and  $\alpha_{hh}$  by interchanging the roles of the relative constitutive constants,  $\epsilon_r$  and  $\mu_r$ , and employing care in observing the resulting signs of the E-field vectors from a knowledge of the H-field vectors. (The right subscript represents the polarization state of the incident wave and the left subscript represents the desired scattered wave.)

1. Bistatic scattering matrix elements for homogeneous surface

$$(23a) \quad \alpha_{hh} = - \frac{(\mu_r - 1)(\mu_r \sin \theta_i \sin \theta_s - \cos \phi_s \sqrt{\epsilon_r \mu_r - \sin^2 \theta_i} \sqrt{\epsilon_r \mu_r - \sin^2 \theta_s}) + \mu_r^2 (\epsilon_r - 1) \cos \phi_s}{[\mu_r \cos \theta_i + \sqrt{\epsilon_r \mu_r - \sin^2 \theta_i}] [\mu_r \cos \theta_s + \sqrt{\epsilon_r \mu_r - \sin^2 \theta_s}]}$$

$$(23b) \quad \alpha_{vh} = \sin \phi_s \cdot \frac{\epsilon_r (\mu_r - 1) \sqrt{\epsilon_r \mu_r - \sin^2 \theta_i} - \mu_r (\epsilon_r - 1) \sqrt{\epsilon_r \mu_r - \sin^2 \theta_s}}{[\mu_r \cos \theta_i + \sqrt{\epsilon_r \mu_r - \sin^2 \theta_i}] [\epsilon_r \cos \theta_s + \sqrt{\epsilon_r \mu_r - \sin^2 \theta_s}]},$$

$$(23c) \quad \alpha_{hv} = \sin \phi_s \cdot \frac{\mu_r (\epsilon_r - 1) \sqrt{\epsilon_r \mu_r - \sin^2 \theta_i} - \epsilon_r (\mu_r - 1) \sqrt{\epsilon_r \mu_r - \sin^2 \theta_s}}{[\epsilon_r \cos \theta_i + \sqrt{\epsilon_r \mu_r - \sin^2 \theta_i}] [\mu_r \cos \theta_s + \sqrt{\epsilon_r \mu_r - \sin^2 \theta_s}]},$$

$$(23d) \quad \alpha_{vv} = \frac{(\epsilon_r - 1)(\epsilon_r \sin \theta_i \sin \theta_s - \cos \phi_s \sqrt{\epsilon_r \mu_r - \sin^2 \theta_i} \sqrt{\epsilon_r \mu_r - \sin^2 \theta_s}) + \epsilon_r^2 (\mu_r - 1) \cos \phi_s}{[\epsilon_r \cos \theta_i + \sqrt{\epsilon_r \mu_r - \sin^2 \theta_i}] [\epsilon_r \cos \theta_s + \sqrt{\epsilon_r \mu_r - \sin^2 \theta_s}]}$$

In the above expressions,  $\epsilon_r$  and  $\mu_r$ , the relative surface material permittivity and permeability, may each be either real or complex (indicating lossless or lossy material), and be either greater, equal to, or less than unity in magnitude.

2. Backscattering matrix elements for homogeneous surface

The above elements are readily reduced to the case of back-scattering where  $\phi_s = \pi$  and  $\theta_s = \theta_i$ .

$$(24a) \quad \alpha_{hh} = - \frac{(\mu_r - 1) [(\mu_r - 1) \sin^2 \theta_i + \epsilon_r \mu_r] - \mu_r^2 (\epsilon_r - 1)}{[\mu_r \cos \theta_i + \sqrt{\epsilon_r \mu_r - \sin^2 \theta_i}]^2}$$

$$(24b) \quad \alpha_{vh} = \alpha_{hv} = 0,$$

and

$$(24c) \quad \alpha_{vv} = \frac{(\epsilon_r - 1) [(\epsilon_r - 1) \sin^2 \theta_i + \epsilon_r \mu_r] - \epsilon_r^2 (\mu_r - 1)}{[\epsilon_r \cos \theta_i + \sqrt{\epsilon_r \mu_r - \sin^2 \theta_i}]^2}$$

3. Bistatic scattering matrix elements  
for perfectly conducting surface

The scattering matrix elements for a perfectly conducting surface may be readily determined from Eqs. (23) by putting  $\mu_r = 1$  and  $\epsilon_r \rightarrow \infty$ ;\* this is evident from consideration of the basic boundary conditions for the two cases.

$$(25a) \quad \alpha_{hh} = -\cos \phi_s ,$$

$$(25b) \quad \alpha_{vh} = -\frac{\sin \phi_s}{\cos \theta_s} ,$$

$$(25c) \quad \alpha_{hv} = +\frac{\sin \phi_s}{\cos \theta_i} ,$$

$$(25d) \quad \alpha_{vv} = \frac{\sin \theta_i \sin \theta_s - \cos \phi_s}{\cos \theta_i \cos \theta_s} .$$

4. Backscattering matrix elements for  
perfectly conducting surface

Here again, we set  $\phi_s = \pi$  and  $\theta_s = \theta_i$  in the above equations.

$$(26a) \quad \alpha_{hh} = 1 ,$$

$$(26b) \quad \alpha_{vh} = \alpha_{hv} = 0 ,$$

$$(26c) \quad \alpha_{vv} = \frac{1 + \sin^2 \theta_i}{\cos^2 \theta_i} .$$

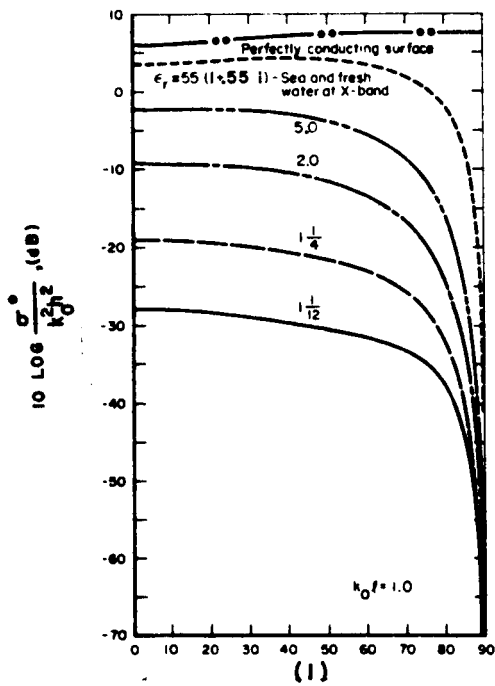
---

\* Actually, a perfectly conducting surface implies that the imaginary part of  $\epsilon_r$  approaches infinity; the same result is obtained for either limit, however.

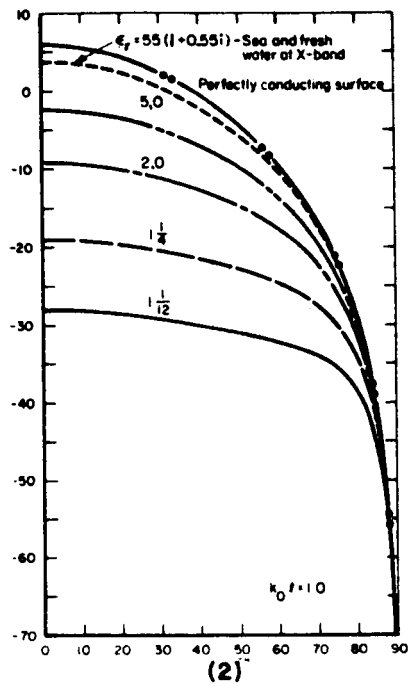
The average incoherent scattering cross section per unit surface area is now obtained using Eqs. (19) along with the proper scattering matrix elements,  $\alpha_{Y\bar{Y}}$ , for the desired combination of vertical and horizontal polarization states. These are given above. The factor  $I$  used in Eq. (19a) is given in terms of the surface roughness spectral density, as discussed previously and shown in Eq. (19b).

Two outstanding facts are in evidence from the above equations for the important case of radar backscattering. For one thing, the cross polarized components are zero. It should be pointed out, however, that these components, as indicated above, are zero only to the first order. The next order neglected terms in  $\sigma_{YH}^0$  and  $\sigma_{HY}^0$  are proportional to the mean square height and slope,  $k_o^2 h^2$  and  $s^2$ , with respect to  $\sigma_{HH}^0$  and  $\sigma_{VV}^0$ . An expression for these terms is derived by Valenzuela (1967). The lowest order terms retained here vary with  $k_o^4$ , while the next order terms derived by Valenzuela are of order  $k_o^6$  in frequency. Thus our results indeed represent the solution in the low frequency limit. The second fact is that backscatter differs for the vertical and horizontal states. The vertical component is always greater than the horizontal for  $|\epsilon_r| > |\mu_r|$ , except at normal incidence where they are equal (i.e.,  $\theta_i = 0$ ). This fact has been observed experimentally, but previous theories based upon the less accurate tangent plane approximation have failed to show any such difference. (Davies, *ibid.*).

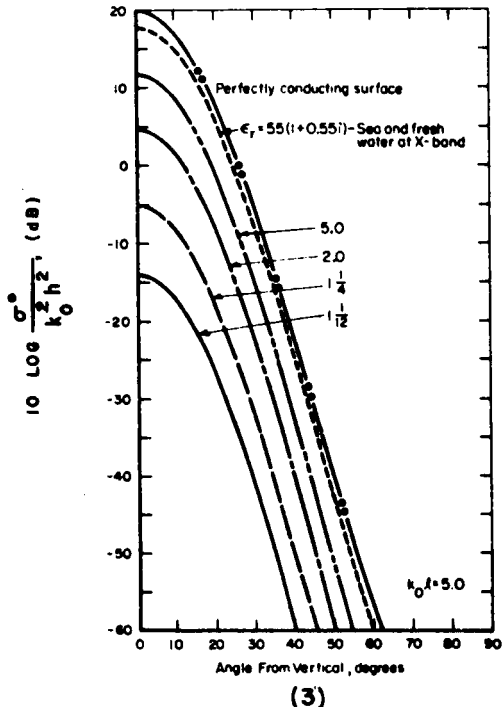
Plots showing the average incoherent backscattering cross section per unit surface area are presented in Fig. 2 for perfectly conducting surfaces along with dielectric surfaces. The cross sections for both vertical and horizontal polarization states are given. These cross sections are normalized by dividing by  $k_o^2 h^2$ . The Gaussian correlation coefficient model given above was used with two relative correlation lengths (i.e.,  $k_o \ell = 1.0$  and  $k_o \ell = 5.0$ ). The results for  $k_o \ell < 1.0$  are not significantly different in shape from those for  $k_o \ell = 1.0$ , but the magnitude of the cross section itself varies in direct proportion to  $k_o^2 \ell^2$ , as seen from Eqs. (19a), (20), and (22). Note that as correlation length (i.e.,  $k_o \ell$ ) increases, more of the backscattered power is concentrated near the specular direction at normal incidence and less near grazing. This is physically reasonable, because surfaces with a given mean roughness height,  $h^2$ , are smoother when the roughness height correlation length,  $\ell$ , is longer. This can be seen from Eq. (21) for the mean square slope of a rough surface.



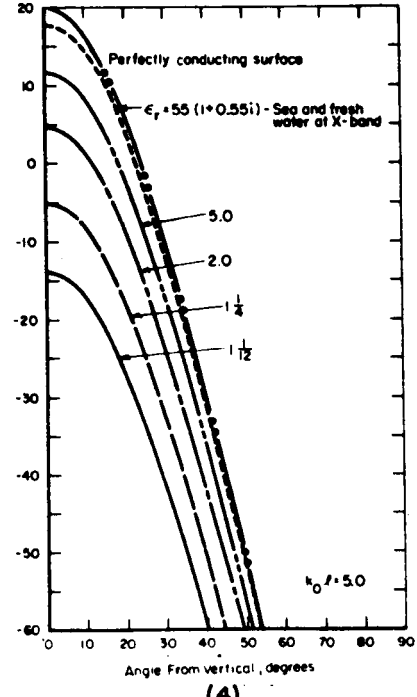
(1)



(2)



(3)



(4)

Fig. 2. Average incoherent backscattering cross sections per unit area with linear polarization states from slightly rough surface model vs. incidence angle for Gaussian surface height correlation coefficients, normalized to  $k_0^2 h^2$ .  
 (1)  $k_0 l = 1$ , vertical polarization states, (2)  $k_0 l = 1.0$ , horizontal polarization states, (3)  $k_0 l = 5.0$ , vertical polarization states, (4)  $k_0 l = 5.0$ , horizontal polarization states.

#### D. Results for Circular Polarization States

It is relatively easy to transform from the vertical and horizontal polarization states to the circular polarization states by using standard matrix methods. As mentioned previously, the elements  $\alpha_{vv}$ ,  $\alpha_{hh}$ ,  $\alpha_{vh}$ , and  $\alpha_{hv}$  are directly proportional to scattering matrix elements, preserving both proper relative amplitudes and phase differences. Hence, a set of analogous elements applicable for circular polarization are determined and given below for use in Eq. (19a).

##### 1. Bistatic scattering matrix elements<sup>\*</sup>

$$(27a) \quad \alpha_{LR} = \frac{\alpha_{hh} + \alpha_{vv} + i(\alpha_{hv} - \alpha_{vh})}{2} ,$$

$$(27b) \quad \alpha_{RR} = \frac{\alpha_{hh} - \alpha_{vv} + i(\alpha_{hv} + \alpha_{vh})}{2} ,$$

$$(27c) \quad \alpha_{RL} = \frac{\alpha_{hh} + \alpha_{vv} - i(\alpha_{hv} - \alpha_{vh})}{2} ,$$

$$(27d) \quad \alpha_{LL} = \frac{\alpha_{hh} - \alpha_{vv} - i(\alpha_{hv} + \alpha_{vh})}{2} .$$

The quantities on the right side of these equations are given in Eqs. (23) for a homogeneous surface material or by Eqs. (25) for a perfectly conducting surface.

---

\* The right subscript represents the polarization state of the incident wave and the left subscript represents that of the desired scattered wave.

## 2. Backscattering matrix elements

In the case of backscattering, it was shown in Eqs. (24) that  $\alpha_{vh} = \alpha_{hv} = 0$ . Hence the above elements reduce to the following:

$$(28a) \quad \alpha_{LR} = \alpha_{RL} = \frac{\alpha_{hh} + \alpha_{vv}}{2} \quad ,$$

$$(28b) \quad \alpha_{LL} = \alpha_{RR} = \frac{\alpha_{hh} - \alpha_{vv}}{2} \quad .$$

In this case, the elements on the right side are given by Eqs. (24) for a homogeneous surface material and by Eq. (26) for a perfectly conducting surface.

Physically,  $\alpha_{RL}$  and  $\alpha_{LR}$  represent the "polarized" components in the scattered field; for backscattering from a smooth surface or symmetric object, the scattered circular state is always opposite sense from that of the incident circular state. "Depolarization", then, appears in the elements  $\alpha_{LL}$  and  $\alpha_{RR}$ , representing the scattered circular state of the same sense as the incident state. It is important to note that depolarization occurs for the circular states for backscattering even though it does not occur for the linear states (i.e.,  $\alpha_{hv} = \alpha_{vh} = 0$ ); this is due to the non-zero difference between  $\alpha_{hh}$  and  $\alpha_{vv}$ .

Curves showing the normalized average backscattering cross section per unit surface area as a function of incidence angle are presented in Fig. 3. These represent perfectly conducting and dielectric surfaces for both the "polarized" and "depolarized" components. The Gaussian surface height correlation coefficient model is used with two values of the correlation length,  $k_o l = 1.0$  and  $5.0$ . It must be emphasized again that all of these curves were derived from a first-order perturbation theory; higher order terms in  $k_o h$  and  $s$  (relative rms roughness height and slope) have been neglected.

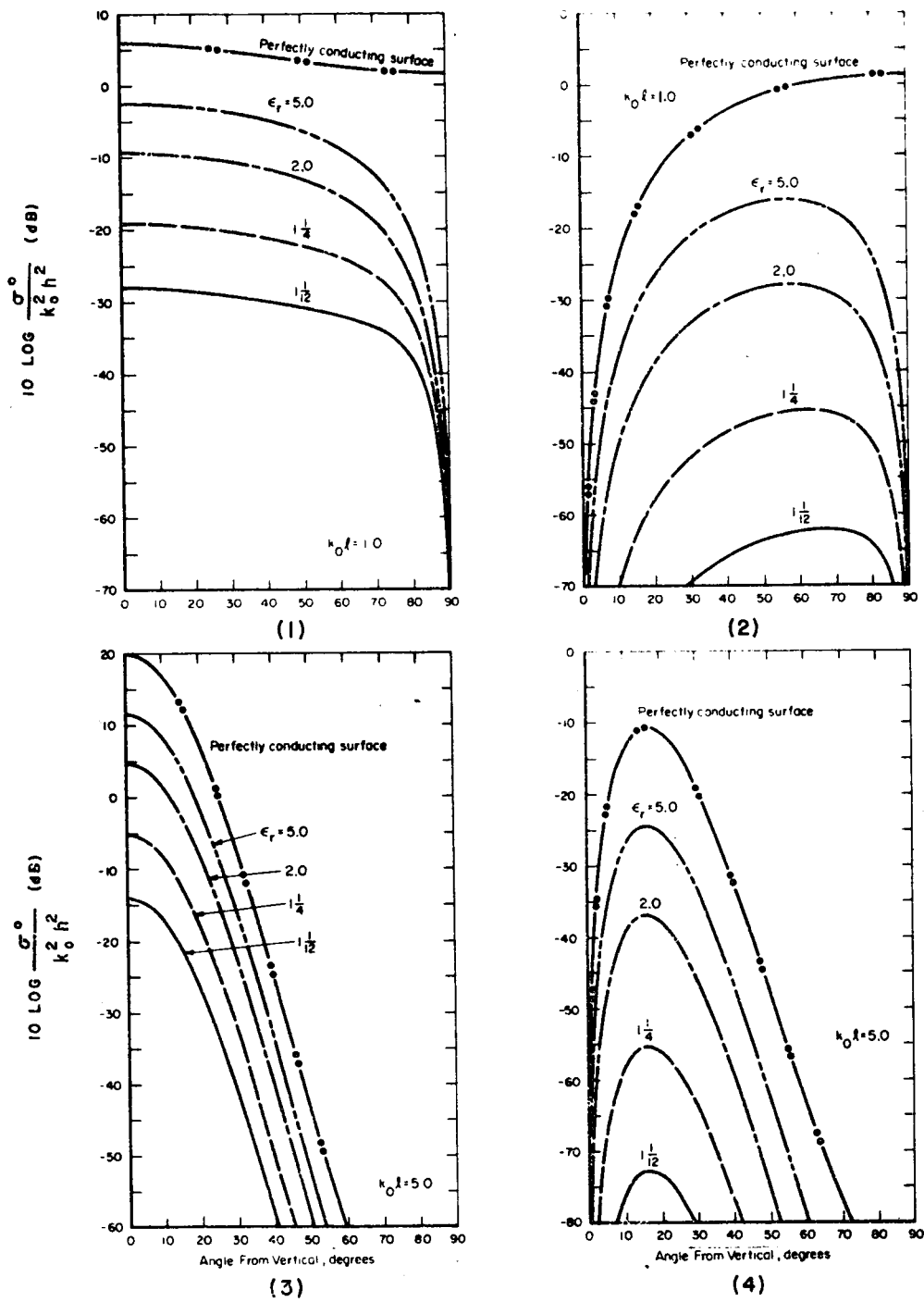


Fig. 3. Average incoherent backscattering cross sections per unit area with circular polarization states from slightly rough surface model vs. incidence angle for Gaussian surface height correlation coefficient, normalized to  $k_0^2 h^2$ . (1)  $k_0\ell = 1.0$ , opposite sense polarization states, (2)  $k_0\ell = 1.0$ , same sense polarization states, (3)  $k_0\ell = 5.0$ , opposite sense polarization states, (4)  $k_0\ell = 5.0$ , same sense polarization states.

## E. Results for Arbitrary Linear Polarization States

In many experimental situations, the transmitting and receiving antennas employ linear polarization states, but they may not necessarily be oriented along either the vertical or the horizontal polarization directions defined by the surface coordinate system. Define  $\eta_i$  as the angle between the unit vector  $\hat{\theta}_i$  and the desired incident E-field component in the direction toward the unit vector  $\hat{\phi}_i$ . Define  $\eta_s$  in the same way with respect to  $\hat{\theta}_s$  and  $\hat{\phi}_s$ . Then the matrix element  $\alpha_{\eta_s \eta_i}$  for bistatic scattering can be written

$$(29) \quad \alpha_{\eta_s \eta_i} = \alpha_{vv} \cos \eta_i \cos \eta_s + \alpha_{vh} \sin \eta_i \cos \eta_s \\ + \alpha_{hv} \cos \eta_i \sin \eta_s + \alpha_{hh} \sin \eta_i \sin \eta_s .$$

### 1. Backscattering with aligned and crossed linear polarized antenna

Often the transmitter and receiver antennas are aligned so that  $\eta_s = \eta_i$ . For the receiver antenna polarization direction orthogonal to this,  $\eta_s = \eta_i + \pi/2$ . Employing these angles and also the fact that  $\alpha_{vh} = \alpha_{hv} = 0$  for backscattering, we arrive at the following two elements:

$$(30a) \quad \alpha_{\eta_i \eta_i} = \alpha_{vv} \cos^2 \eta_i + \alpha_{hh} \sin^2 \eta_i ,$$

and

$$(30b) \quad \alpha_{\eta_i + \pi/2, \eta_i} = -(\alpha_{vv} - \alpha_{hh}) \sin \eta_i \cos \eta_i .$$

These elements can be used in Eq. (19a) to determine the backscattering cross section. The elements  $\alpha_{hh}$  and  $\alpha_{vv}$  to be used in the right side of the above are given in Eqs. (24) for a homogeneous surface material and Eq. (26) for a perfectly conducting surface.

## 2. Angularly averaged backscattering with aligned and crossed linear polarized antennas

In many cases aligned and crossed linear transmitting and receiving antennas may be employed, but the antenna angle,  $\eta_i$ , with respect to the surface vertical may be rotating and unknown at a given instant of time. This may arise in the case of satellite observations of a planetary surface. In other situations it can result from uncontrollable Faraday rotation of polarization due to the ionosphere. Another situation where an average quantity is desired is the case where a relatively short pulse of linear polarization sweeps past a planetary surface, illuminating an annular portion of the sphere. The angle,  $\eta_i$ , between the linear direction and the local plane of incidence at a given point on the annulus varies continuously between 0 and  $2\pi$  in this case.

In the above cases, the quantities desired are  $|\alpha_{\eta_i \eta_i}|^2$  and  $|\alpha_{\eta_i + \pi/2, \eta_i}|^2$ , averaged by integrating over  $\eta_i$  from 0 to  $2\pi$  and dividing by  $2\pi$ . These quantities become

$$(31a) \quad \langle |\alpha_{\eta_i \eta_i}|^2 \rangle = \frac{1}{8} [3|\alpha_{vv}|^2 + 2\text{Re}(\alpha_{vv}\alpha_{hh}) + 3|\alpha_{hh}|^2] ,$$

and

$$(31b) \quad \langle |\alpha_{\eta_i + \pi/2, \eta_i}|^2 \rangle = \frac{|\alpha_{vv} - \alpha_{hh}|^2}{8} .$$

The notation  $\text{Re}(x)$  denotes the real part of  $x$ .

## F. Comparison with Measured Results

It is difficult to find measured data with which to compare the preceding theoretical results for a slightly rough surface for two reasons. (i) It is necessary that roughness height be everywhere small compared to wavelength. (ii) It is difficult experimentally to separate the average coherent scattered power from the incoherent; in most cases, no attempt is made to do this. For backscattering, the coherent contribution to the total power dominates near normal incidence. The results presented in this section apply only to the incoherent scattered power.

Recently, average backscattering cross section measurements were reported by Wright (1966) from a fresh water surface at X-band.

Capillary waves were generated under controlled conditions such that the wave amplitudes were small compared to radar wavelength. Return for the both vertical and horizontal states were obtained, and are shown in Fig. 4 as a function of incidence angle. Along with these measured curves, theoretical curves are drawn, using the equations derived above and the parameters of the water surface estimated by Wright. These are  $\epsilon_r = 55(1 + i.55)$ ,  $k_0 h = .05$ ,  $k_0 l = 2$ . It should be noted that the measured results were presented not in terms of backscattering cross section per unit area, but backscattering cross section in square meters. Since the area of the illuminated surface was not given, the absolute value of  $\sigma_{vv}^0$  and  $\sigma_{hh}^0$  cannot be ascertained. Hence, the magnitudes shown in the figure are made to conform to the theoretical. The significant observation is the agreement in functional dependence between the measured and theoretical curves.

Another set of measurements on an asphalt surface at X- and  $K_a$ -bands allow another comparison with the model. (See Fig. 5). Actual measurements of surface statistics and dielectric constant were made in this case and used to compute the curves for the slightly rough surface model, (Cosgriff, 1960). Again the functional dependence on frequency, angle, and polarization is in good agreement. Even the somewhat poorer agreement in absolute value is reasonable in view of the large number of surface parameters which had to be estimated from rather small samples.

### III. VERY ROUGH PLANAR SURFACE

#### A. Introduction

The remaining class of rough surfaces which can be treated analytically is the one whose members have a large scale roughness such that the local surface radii of curvature over nearly all surface regions are much greater than wavelength. In most cases of practical interest, the rms roughness height,  $h$ , will then also be larger than a wavelength. Then all of the scattered power from such a surface is incoherent. (i.e., the phase angle of the scattered field becomes uniformly distributed between 0 and  $2\pi$ , and hence the average value of the scattered field is zero; only the average scattered power is non-zero.)

When this radius of curvature criterion is satisfied, the scattering problem can be solved by several optics techniques. If these are used properly, they all lead to the same result. The value of examining more than one approach to the problem lies in the physical insight into

Fig. 4. Measured average back-scattering cross section per unit area from slightly rough fresh water surface at X-band vs. incidence angle for vertical and horizontal polarization states. Dashed curves represent slightly rough surface model using parameters measured from fresh water surface.

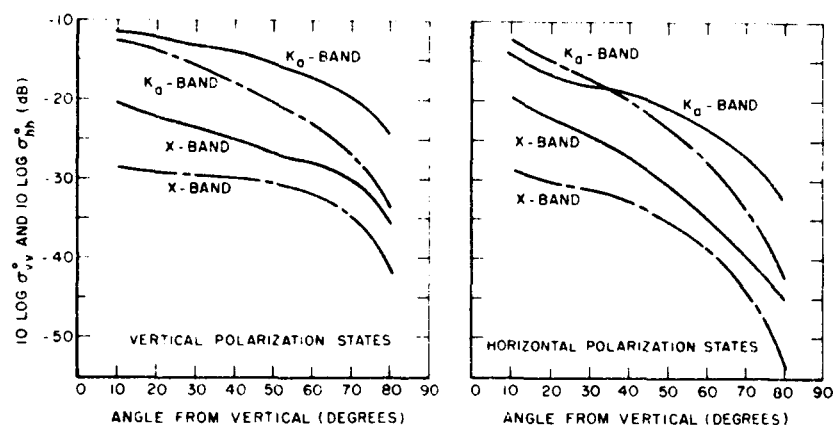
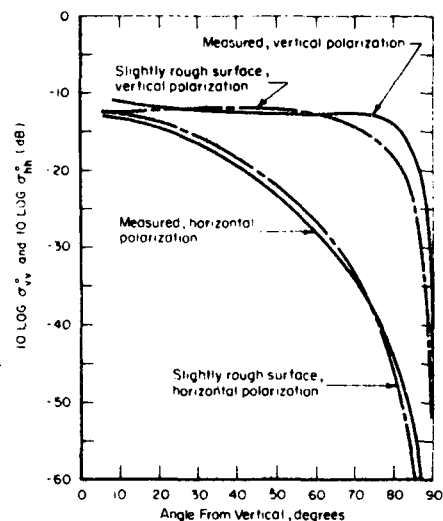


Fig. 5. Measured average backscattering cross section per unit area from slightly rough asphalt surface at X- and Ka-bands vs. incidence angle for linear polarization states. Dashed curve is slightly rough surface model using measured parameters  $\rho(r) = (1+20r^2)^{-3/2}$ , where  $r$  is in cm;  $k_0 l \approx 0.085$  at X-band and 0.30 at Ka-band;  $k_0 l \approx 0.48$  at X-band and 1.7 at Ka-band;  $\epsilon_r \approx 4.3 + i0.1$  at X-band and  $2.5 + i0.65$  at Ka-band.

the scattering process which each provides. At present, three different optics approaches have appeared in the literature. Rather than retrace a derivation in detail here, a critique of these existing analyses will be made, along with the physical explanation of each. Finally, the common results of these analyses will be presented and curves for two models will be shown for comparison.

All of the three optics approaches apply to the class of rough surfaces which satisfy (at least) the following restrictions:

- (a) The local surface radii of curvature at nearly every point on the surface are considerably larger than wavelength.
- (b)  $\partial\zeta/\partial x, \partial\zeta/\partial y < 1.0$ , i.e., surface slopes are relatively small. Only when this is true can one neglect shadowing and multiple scattering over most of the range of incidence and scattering angles.
- (c)  $\langle(\partial\zeta/\partial x)^2\rangle = \langle(\partial\zeta/\partial y)^2\rangle$ , i.e., the roughness is isotropic. The restriction is not necessary to obtain an answer, but is employed in this paper for simplicity.
- (d)  $L > > \ell > > \lambda$ , i.e., the dimensions of the illuminated area are much greater than the roughness correlation length,  $\ell$ , which in turn is much greater than wavelength. The second portion of the inequality is automatically fulfilled if (a) is true. The first part of the inequality precludes the possibility of looking at only a part of a hill or wave, but rather it demands that several hills or waves be included in the illuminated area.
- (e)  $k_0^2 h^2 > > 1$ , i.e., mean square roughness height,  $h^2$ , is of the order of, or greater than, wavelength squared.
- (f) The surface height correlation coefficient,  $\rho(r)$ , must be parabolic in behavior at the origin, i.e.,  $\rho(r) \xrightarrow[r \rightarrow 0]{} 1 - r^2/\ell^2$ , where  $r$  is the separation between two points on the surface and  $\ell$  is termed here the correlation length.

The first two restrictions above permit use of the tangent plane (or physical optics) approximation. This approximation involves writing the scattered field at the surface as the product of the incident field and the proper reflection coefficient. Restriction (f) is imposed in order to avoid mathematical difficulties which lead to erroneous results when one employs a correlation coefficient whose behavior is linear at the origin, (Barrick, 1968). The second, third and fourth restrictions are identical to those given previously for the slightly rough surface.

Although the slightly rough surface analysis of the preceding part takes into account multiple scattering and shadowing, the normal optics techniques used for very rough surfaces ignore these multiple interaction effects. Generally, they are higher-order effects so long as the surface slopes are not too precipitous and the scattering angles are not too close to grazing. No known correction factor for multiple scattering has been computed, but shadowing corrections have been formulated recently. Beckmann (1965) first formulated the "shadowing function." This was later revised by Brockelman and Hagfors (1966) and Wagner (1967). The latter shows that the correction factor is less than 3 dB for angles of incidence and scattering more than  $10^\circ$  above grazing and an rms total surface slope,  $\tan^{-1}s = \tan^{-1}(2h/l)$ , of less than  $27^\circ$ . In view of the restrictions placed upon the class of surfaces considered here, shadowing corrections will not be introduced in this paper.

## B. Review and Interpretation

### 1. Physical optics approach

The first approach to appear historically is also probably the most mathematically thorough and satisfying. By the same token, it probably sheds the least physical insight on the scatter mechanism because of the mathematical detail. This method employs a physical optics integral expression for the scattered field. The total fields at the surface appearing in the integrand are determined from the tangent plane approximation mentioned above. The first comprehensive treatment of this problem for a perfectly conducting surface was made by Isakovitch (1952) who employed a vector physical optics formulation. This work appears to have been overlooked by Western investigators, for Davies (1954) solves the same problem by the same techniques, but employs a less complete scalar formulation. Beginning about 1960, a variety of Western and Soviet investigators began to extend these results. Among these are Hagfors (1960, 1964), Beckmann (1963), Hughes (1962), Fung (1964), Hayre (1961), Daniels (1961), Semenov (1965), and Stogryn (1967). Semenov appears to have been the first to have solved the problem for scattering from a surface of homogeneous material,  $\epsilon_r, \mu_r$ , using a vector formulation, which accounts properly for polarization. The results of Semenov have been derived independently and simultaneously by Barrick, and the two are in agreement, after some algebraic simplification of Semenov's results. Stogryn's solution is the same as that of Semenov (although his notation is more complicated), and hence serves as a third check on Semenov's analysis.

Semenov expresses the scattered vector field (for both vertical and horizontal incident polarization directions) in terms of a physical optics integral. For example, for an incident plane wave whose E-field is horizontally polarized, the integral, after application of the tangent plane approximation, can be written as follows: (See Fig. 1).

$$(32) \quad \bar{E}^s = - \frac{ik_o e^{ik_o R_o}}{4\pi R_o} E_h^i \int_{-L/2}^{L/2} \int_{-L/2}^{L/2} \bar{F}(\zeta_x, \zeta_y) e^{ik_o [\hat{k}_i - \hat{k}_s] \cdot \bar{r}} dx dy,$$

where

$R_o$  = distance from origin to observation point,

$\bar{r} = x \hat{x} + y \hat{y} + \zeta(x, y) \hat{z}$  = distance from origin to point on rough surface,

$\hat{k}_i, \hat{k}_s$  - unit constant vectors pointing in direction of incidence and scattering,

$\zeta_x, \zeta_y$  - local surface slopes in  $x$  and  $y$  directions at surface point  $\zeta(x, y)$ , i.e.,  $\partial\zeta/\partial x$  and  $\partial\zeta/\partial y$ .

The factor  $\bar{F}(\zeta_x, \zeta_y)$  is a function of the local normal to the surface and of the local Fresnel reflection coefficients at each surface point. It can be expressed as follows:

$$(33a) \quad \bar{F}(\zeta_x, \zeta_y) = \frac{\sqrt{1 + \zeta_x^2 + \zeta_y^2}}{\sin^2 \gamma_i} \cdot [\hat{y} \cdot (\hat{k}_i \times \hat{n}) \bar{G}_\perp + \hat{y} \cdot (\hat{k}_i \cos \gamma_i + \hat{n}) \bar{G}_\parallel],$$

where

$$(33b) \quad \bar{G}_\perp = [\cos \gamma_i - \cos \gamma_s R_\perp(\gamma_i)] [(\hat{k}_i \times \hat{n}) - \hat{k}_s \cdot (\hat{k}_i \times \hat{n}) \hat{k}_s] + [1 + R_\perp(\gamma_i)] \hat{k}_s \times (\hat{k}_i + \hat{n} \cos \gamma_i),$$

$$(33c) \quad \bar{G}_\parallel = [1 + R_\parallel(\gamma_i)] [(\hat{k}_i + \hat{n} \cos \gamma_i) - \hat{k}_s \cdot (\hat{k}_i + \hat{n} \cos \gamma_i) \hat{k}_s] + [\cos \gamma_i - \cos \gamma_s R_\parallel(\gamma_i)] [\hat{k}_i \cos \gamma_s - (\hat{k}_s \cdot \hat{k}_i) \hat{n}],$$

$$(33d) \quad \hat{n} = \frac{-\zeta_x \hat{x} - \zeta_y \hat{y} + \hat{z}}{\sqrt{1 + \zeta_x^2 + \zeta_y^2}} = \text{local unit normal vector to surface at point } \zeta(x, y),$$

$\gamma_i, \gamma_s$  - local incidence and scattering angles in planes of incidence and scattering with respect to local surface normal, (i.e.,  $\cos \gamma_i = -\hat{k}_i \cdot \hat{n}$ ,  $\cos \gamma_s = \hat{k}_s \cdot \hat{n}$ ),

$R_{\perp}(\gamma_i), R_{\parallel}(\gamma_i)$  - Fresnel reflection coefficients at local surface point  $\zeta(x, y)$  with incidence angle,  $\gamma_i$ .

As one can observe, the integrand consists of the factor  $\bar{F}(\zeta_x, \zeta_y)$ , which varies with the local surface slopes from point to point on the surface, and an exponential phase factor containing the phase difference between the local surface point and the scattered field point. The first factor is to be removed from the integrand as a constant; the justification for this is the stationary phase (or specular point) argument. This argument maintains that for large  $k_0$  in the exponential factor, the only surface regions which contribute to the integral are those smoothly curving portions which are in a position to specularly reflect into the desired scattering direction. The direction of the surface normal,  $\hat{n}_{sp}$ , and the local incidence angle,  $\gamma_i = \gamma_s = \iota$ , at these specular points are readily determined by bisecting the angle between the incidence propagation direction and the desired scattering propagation direction. The constant factor,  $F(\zeta_{x_{sp}}, \zeta_{y_{sp}})$ , is then evaluated using the slopes of the surface at these specular points.

The remaining integral containing the exponential phase factor is not solved by the same specular point or stationary phase approach, however; the scattered field is squared to give scattered power or intensity, and then it is averaged. Averaging consists of multiplying the double integral by the joint probability density functions for the surface height at two different surface points and then integrating over these two random variables. The order of integration is interchanged, and the integrand of the former double integral is averaged first. This interchange is justified mathematically (See Middleton, 1960) so long as restriction (f) is applied. With the aid of restriction (e), the remaining integral is solved in a straightforward manner; nearly all of the above mentioned references carry out this latter process correctly.

The step of averaging under the integral sign, though mathematically correct, obscures the physical understanding of the scattering mechanism. It is also somewhat less than satisfying to justify the removal of a complicated factor in the integrand by the specular point or stationary phase argument, but then never to actually employ this stationary phase principle to solve the remaining integral. However, the two approaches to be discussed subsequently do justify the validity of this procedure by actually showing that the specular point theories give exactly the same result, at least for a Gaussian distributed surface height.

No one has yet justified correctly a more exact method of evaluating this integral than the stationary phase approach. This is obviously due to

the extremely complicated form of the factor  $\bar{F}(\zeta_x, \zeta_y)$ . At least two previous analyses have proposed alternate schemes for evaluating the integral. Barrick (1965) suggested averaging this factor independent of the exponential factor; hence,  $\bar{F}(\zeta_x, \zeta_y)$  would be removed as a constant evaluated at the mean slopes, i.e.,  $\bar{F}(0, 0)$ . Fung (1965) proposed expanding the factor in a series in  $\zeta_x$ ,  $\zeta_y$ , and averaging each term separately. One can show that the resultant series cannot be truncated, since higher order terms are of the same order as the first terms. This is true even for vanishingly small values of surface slopes,  $\zeta_x$  and  $\zeta_y$ . Both of these approaches are inconsistent with the stationary phase principle, and therefore both can have no theoretical justification.

Recently, Kivelson and Moszkowski (1965) have shown that for backscattering one can reduce the physical optics integral directly to the probability density function for the surface normal; this thus provides a valuable connection to the ray optics approach of the next section. Gaussian surface statistics are not necessary for their analysis, but the generalized form selected for their conditional surface height probability density function is still somewhat restrictive. The joint probability density function which they form is then not symmetric in the two height random variables,  $\zeta$  and  $\zeta'$ , as it must be, except for the special case of Gaussian statistics.

## 2. Ray optics approach

Recently, Muhleman (1964) brought an older - but better understood-theory to bear on the very rough surface problem. The "ray optics" approach (following his terminology) provides a more readily and simply explainable interpretation of the scattering process, even though mathematically it is less exact and elegant. The rough surface is initially approximated by a grid of small flat planar elements, all of which are connected to form the rough surface. Each element reflects incident power specularly, and the direction of reflection from a given facet is determined by the direction of its normal. Hence the amount of power scattered into a given direction is directly proportional to the number of facets whose normals are pointed in the proper direction (i.e., the direction bisecting the angle between the incidence and scattering directions) divided by the total number of facets. This quantity is the probability density function for the surface normal. It is expressible in terms of the probability density function for the surface slopes, since the surface slopes are perpendicular to the local normal.

Muhleman dealt with the problem of bistatic scattering from a perfectly reflecting surface, but the problem of the homogeneous surface

material is just as easily solved. Recall that in the latter case, the components of the local E-field incident upon a planar facet in and perpendicular to the plane of incidence each have different Fresnel reflection coefficients,  $R_{||}$  and  $R_{\perp}$ . Referring to Fig. 1, we can determine the vertical and horizontal reflection coefficients for a properly oriented facet which reflects power incident from direction  $\theta_i$  into direction  $\theta_s, \phi_s$ . Vertical and horizontal here refer to the polarization directions of incident and scattered fields with respect to the mean surface, i.e., the x-y surface, and not with respect to the local surface facet. Let us define  $R_{vh}$  as the reflection coefficient between the horizontally polarized incident (right subscript) and the vertically polarized reflected (left subscript) E-field components with mean incidence and scattering angles  $\theta_i, \theta_s, \phi_s$ . The other three coefficients are defined in the same manner. Then assuming that scattering in these directions is produced by planar facets properly oriented to specularly reflect, these vertical and horizontal reflection coefficients are determined from straightforward geometrical considerations. They are:

$$(34a) \quad R_{hh} = \frac{\sin \theta_i \sin \theta_s \sin^2 \phi_s R_{||}(i) + a_2 a_3 R_{\perp}(i)}{4 \sin^2 i \cos^2 i}$$

$$(34b) \quad R_{vh} = -\sin \phi_s \frac{a_2 \sin \theta_s R_{||}(i) - a_3 \sin \theta_i R_{\perp}(i)}{4 \sin^2 i \cos^2 i}$$

$$(34c) \quad R_{hv} = -\sin \phi_s \frac{a_2 \sin \theta_s R_{\perp}(i) - a_3 \sin \theta_i R_{||}(i)}{4 \sin^2 i \cos^2 i}$$

$$(34d) \quad R_{vv} = -\frac{\sin \theta_i \sin \theta_s \sin^2 \phi_s R_{\perp}(i) - a_3 \sin \theta_i R_{||}(i)}{4 \sin^2 i \cos^2 i},$$

where

$$(35a) \quad R_{||}(\eta) = \frac{\epsilon_r \cos \eta - \sqrt{\epsilon_r \mu_r - \sin^2 \eta}}{\epsilon_r \cos \eta + \sqrt{\epsilon_r \mu_r - \sin^2 \eta}},$$

and

$$(35b) \quad R_{\perp}(\eta) = \frac{\mu_r \cos \eta - \sqrt{\epsilon_r \mu_r - \sin^2 \eta}}{\mu_r \cos \eta - \sqrt{\epsilon_r \mu_r - \sin^2 \eta}},$$

and where  $\iota$  is the local angle of incidence at the specular reflecting facets, and is given by

$$(36) \quad \cos^2 \iota = \frac{1}{2} (1 - \sin \theta_i \sin \theta_s \cos \phi_s + \cos \theta_i \cos \theta_s) .$$

The quantities  $a_2$  and  $a_3$  involve the scattering angles and are given subsequently in Eqs. (54). As a check, the above reflection coefficients for backscattering reduce to the following:

$$(37) \quad R_{hh}, R_{vv} \rightarrow -R_{\parallel}(0), +R_{\perp}(0); \quad R_{hv}, R_{vh} \rightarrow 0.$$

Since polarization differences were not considered by Muhleman, the above quantities squared must be inserted as factors in his results to obtain power scattering for the vertical and horizontal polarization directions as defined in Fig. 1.

Hagfors (1966) showed that the probability density function for surface slopes appearing in Muhleman's result for scattered power can be easily related to the surface height probability density function when the surfaces are Gaussian. In doing so, he showed that for backscattering, one obtains the same result as from the physical optics analysis discussed above. It is readily shown that the two methods are equivalent for bistatic scattering also. [Note, it was pointed out by Hagfors that due to an oversight, one must divide Muhleman's result by the cosine of the angle between the local surface normal and the mean plane normal, i.e., by

$$(38) \quad \cos(\hat{n}, \hat{z}) = \frac{\cos \theta_i + \cos \theta_s}{2 \cos \iota} .$$

The ray optics approach sheds much needed insight into the scattering process from a rough surface. As a rigorous derivation, however, the method can be seriously questioned. Such an approach considers only scattered energy or power, and not the fields themselves; hence phase relationships between fields from different regions are ignored from the outset. The ray optics method assumes specular reflection from a small planar facet in the form of a non-diverging tube or parallel rays. Later when one permits the planar facet to shrink to zero, the paradox between ray optics and modern geometrical optics theory becomes obvious. Diffraction effects and patterns, due to

phase interference, and divergence of rays due to curved phase fronts are ignored. The method, nonetheless, serves our purpose here because, under the restrictions mentioned previously, we are dealing with incoherent scattered power. This means that it is sufficient to add power scattered from different portions of the surface, rather than the fields themselves. Hence ray optics is justified for this problem, and provides needed insight into the scattering process.

### 3. Geometrical optics or stationary phase approach

The third approach is the application of the stationary phase principle to the Kirchoff integral for the complex scattered field. The result shows that scattering from a portion of a quadric curving surface does indeed radiate specularly. The scattering cross sections of such a curved surface is

$$(39) \quad \sigma = \pi |R_1 R_2| ,$$

where  $R_1 R_2$  is the product of the two principal radii of curvature at the specular or stationary phase point. A very rough surface consists of many such specular points. Everyone has observed the dancing specular points on a rippling lake surface on a moonlight night. However, neither of the previous theories directly relate the total scattered power to the number of specular points and their radii of curvature, even though the physical optics method justifies the simplification of the integrand on the basis that this stationary phase principle is valid. It is therefore instructive to examine the scattering problem formulated on this basis and note that one arrives at the same result as the preceding two approaches. In addition, this third technique provides further insight by explicitly deriving the average number of specular points on a rough surface and their average Gaussian curvature,  $R_1 R_2$ .

Kodis (1966) formulated the rough surface problem rigorously in this manner and showed by stationary phase that the scattering cross section for a rough surface can be expressed, as one intuitively expects, as follows:

$$(40) \quad \sigma = \left\langle \pi \sum_{i,j=1}^N (|R_{1i}R_{2i}| \cdot |R_{1j}R_{2j}|)^{\frac{1}{2}} e^{i(\phi_i - \phi_j)} \right\rangle$$

where the total number of specular points is  $N$  and the Gaussian curvature at the  $i$ -th points is  $R_{1i}R_{2i}$ . The quantity  $\phi_i - \phi_j$  contains the path length difference between the  $i$ -th and  $j$ -th specular points. Employing the restriction  $\rho, h > \lambda$ , one can show that for a very rough surface, the specular points are randomly and widely separated in terms of wavelength, and therefore,  $\phi_i$  and  $\phi_j$  are uniformly distributed. Hence the average scattering cross section becomes

$$(41) \quad \langle \sigma \rangle = \pi \left\langle \sum_{i=1}^N |R_{1i}R_{2i}| \right\rangle .$$

Assuming now that one can assign an average Gaussian curvature to the specular points, one has

$$(42) \quad \langle \sigma \rangle = \pi \langle N \rangle \langle |R_1 R_2| \rangle ,$$

which one expects for incoherent scattering. The average scattering cross section per unit area,  $\sigma_{Y_0}^0$  for incident and scattered polarization states  $\beta$  and  $\gamma$ , can now be expressed

$$(43) \quad \sigma_{Y_0}^0 = \pi n \langle |R_1 R_2| \rangle |R_{Y_0}^{\beta}|^2 ,$$

where

$$(44) \quad n = \frac{\langle N \rangle}{L^2}$$

is the average number of specular points per unit area and  $R_{Y_0}^{\beta}$  is the reflection coefficient for the surface at a specular point. For the vertical and horizontal polarization states (i.e.,  $\gamma, \beta = v, h$ ), these coefficients are given in Eqs. (32).

Barrick (1968) used the above formulation and obtained expressions for  $n$  and  $\langle |R_1 R_2| \rangle$ . These results are identical to those of the previous two approaches. While confirming the general validity of and similarity among the various high frequency optics techniques applied rough surfaces this third approach also provides valuable insight into the scattering process, which is complementary to that of the other two. In

particular, one finds that the average number of specular points is proportional to the probability density function for the surface slopes evaluated at the required slopes at the specular point; this quantity is greatest where the local normal at the specular points (or bisector between incidence and scattering directions) is near the mean normal, or vertical. This is reasonable from consideration of the moonlit lake example. The mean value of the radii of curvature product at the specular points, on the other hand, becomes greater as the local normal is farther removed from the mean normal.

### C. Results

#### 1. General form

Since the solutions for all three approaches are essentially the same for the Gaussian surface, we shall present one result here. It is expressed in a form which proceeds naturally from the physical optics approach and is obtained from the derivation of Semenov (1965). The average scattering cross section per unit surface area, for incident polarization state  $\delta$  and scattered state  $\gamma$ , is written as follows:

$$(45) \quad \sigma_{\gamma\delta}^0 = |\beta_{\gamma\delta}|^2 J .$$

The quantity  $\beta_{\gamma\delta}$  has exactly the same significance as  $\alpha_{\gamma\delta}$  for the slightly rough surface model: it is directly proportional to the scattering matrix element relating the incident field of polarization state  $\delta$  to the scattered field component of polarization state  $\gamma$ . These quantities will be given below for the vertical and horizontal as well as circular states.

The factor  $J$  is related to the roughness statistics in the following manner:

$$(46) \quad J = 2k_o^2 \int_0^\infty r J_o(tr) M_{\zeta\zeta'}(iu, -iu; r) dr .$$

The quantity  $t$  is a function of the scattering angles and is given in Eq. (19c). The symbol  $u$ , also a function of these angles, is defined as

$$(47) \quad u = k_o(\cos \theta_i + \cos \theta_s) .$$

The function  $M_{\zeta\zeta'}(iu, iv; r)$  is the characteristic function of the surface height random variables  $\zeta$  and  $\zeta'$ , measured at surface points  $(x, y)$  and  $(x', y')$ . (Formally, it is the double Fourier transform of the joint probability density function,  $P(\zeta, \zeta'; r)$ ;  $r$  is the horizontal distance between the surface points;

$$(48) \quad r = \sqrt{(x-x')^2 + (y-y')^2} .$$

Therefore, in order to obtain a closed form result for the scattering cross section, one must either know or assume a form for the surface height joint probability density function. (For the slightly rough surface, recall, one has to choose a form for the surface height correlation coefficient.) We shall select two common probability density function models for the sake of comparison and find the quantity  $J$ .

a. Gaussian surface height joint probability density

Using the standard Gaussian joint probability density function

$$(49) \quad P_G(\zeta, \zeta') = \frac{1}{2\pi h^2 [1 - \rho^2(r)]^{\frac{1}{2}}} e^{-\frac{[\zeta^2 - 2\zeta\zeta'\rho(r) + \zeta'^2]}{2h^2[1 - \rho^2(r)]}} ,$$

along with restriction (f) on the form of the correlation coefficient  $\rho(r)$  near the origin and restriction (e) on the size of the mean square roughness height,  $h^2$ , compared to wavelength, we can readily solve Eq. (46) for  $J$ .

$$(50) \quad J = \frac{4}{s^2 u^2} e^{-\frac{1}{s^2} \frac{t^2}{u^2}} ,$$

where

$$s^2 = \frac{4h^2}{\ell^2}$$

is the total mean square slope of the rough surface.

b. Exponential surface height  
joint probability density

For the sake of comparison with the preceding model, we select an exponential probability density model of the following form:

$$(51) \quad PE(\zeta, \zeta') = \frac{3}{2\pi h^2 [1 - \rho^2(r)]^{\frac{1}{2}}} e^{-\left\{ \frac{\zeta^2 - 2\zeta\zeta' \rho(r) + \zeta'^2}{\frac{1}{3} h [1 - \rho^2(r)]} \right\}^{\frac{1}{2}}}.$$

Equation (46) for  $J$  is solved using the same restrictions as with the preceding model.

$$(51) \quad J = \frac{12}{s^2 u^2} e^{-\frac{\sqrt{6}}{s} \frac{t}{u}}.$$

The optics techniques show that for very rough surfaces, the only parameter reflecting the degree of roughness in the scattering cross section is  $s$ , the rms roughness slope. The rms roughness height,  $h$ , does not appear explicitly, and as such is not easily determined from observations of average scattered power from such a surface.

2. Polarization dependence

The elements  $\beta_{\gamma\delta}$  will now be given for several polarization states.

a. Vertical and horizontal states

For the vertical and horizontal polarization states, the scattering matrix elements  $\beta_{vv}$ ,  $\beta_{hh}$ ,  $\beta_{vh}$ , and  $\beta_{hv}$  may be found upon simplification of Semenov's results, or from either of the other two approaches to the problem. They are:

$$(53a) \quad \beta_{vv} = - \frac{\sin \theta_i \sin \theta_s \sin^2 \phi_s R_{\perp}(t) + a_2 a_3 R_{\parallel}(t)}{a_1 a_4}$$

$$(53b) \quad \beta_{hv} = - \sin \phi_s \frac{a_2 \sin \theta_s R_{\perp}(t) - a_3 \sin \theta_i R_{\parallel}(t)}{a_1 a_4}$$

$$(53c) \quad \beta_{vh} = -\sin \phi_s \frac{a_2 \sin \theta_s R_{\perp}(\iota) - a_3 \sin \theta_i R_{\parallel}(\iota)}{a_1 a_4}$$

$$(53d) \quad \beta_{hh} = \frac{\sin \theta_i \sin \theta_s \sin^2 \phi_s R_{\parallel}(\iota) + a_2 a_3 R_{\perp}(\iota)}{a_1 a_4},$$

where  $R_{\parallel}(\iota)$ ,  $R_{\perp}(\iota)$  and  $\iota$  are defined previously in Eqs. (35) and (36) and  $a_1$ ,  $a_2$ ,  $a_3$ ,  $a_4$  are given below.

$$(54a) \quad a_1 = 1 + \sin \theta_i \sin \theta_s \cos \phi_s - \cos \theta_i \cos \theta_s,$$

$$(54b) \quad a_2 = \cos \theta_i \sin \theta_s + \sin \theta_i \cos \theta_s \cos \phi_s,$$

$$(54c) \quad a_3 = \sin \theta_i \cos \theta_s + \cos \theta_i \sin \theta_s \cos \phi_s,$$

$$(54d) \quad a_4 = \cos \theta_i + \cos \theta_s.$$

From the above expressions and the two probability density models previously given, one can substitute the  $\beta$ 's and  $J$  into Eq. (45) to obtain the average scattering cross section per unit area.

b. Circular states and arbitrary polarized linear states

The  $\beta$ 's given above for the vertical and horizontal states, being directly proportional to the scattering matrix elements, can be substituted into Eqs. (27) of the preceding part to give the elements  $\beta_{LR}$ ,  $\beta_{RR}$ ,  $\beta_{RL}$ , and  $\beta_{LL}$  for the circular polarization states. Equations (29) and (30) of that section can be used to give  $\beta_{\eta_i \eta_s}$  for linear polarization states arbitrarily directed.

3. Results for backscattering

Backscattering is the most important and commonly occurring situation for the radar engineer. As such, the above results will be specialized to this case, and curves for the two probability density

models as a function of incidence angle will be presented. The expressions for the  $\beta$ 's given in Eqs. (53) are allowed to approach the backscattering limit (i.e.,  $\theta_s \rightarrow \theta_i$ ,  $\phi_s \rightarrow \pi$ ) to yield

$$(55a) \quad \beta_{vv} = \beta_{hh} \rightarrow - \sec \theta_i R_{||}(0) = \sec \theta_i R_{\perp}(0) ,$$

$$(55b) \quad \beta_{vh} = \beta_{hv} \rightarrow 0 .$$

The circular polarization backscattering matrix elements found from substituting these expressions into Eqs. (27) are

$$(55c) \quad \beta_{LR} = \beta_{RL} = \beta_{vv} = \beta_{hh} \rightarrow \sec \theta_i R_{||}(0) ,$$

$$(55d) \quad \beta_{LL} = \beta_{RR} \rightarrow 0 .$$

The backscattering matrix element between arbitrary linear states as defined and given in Eq. (28) becomes

$$(55e) \quad \beta_{\eta_i \eta_s} = \beta_{vv} \cos(\eta_s - \eta_i) = - \sec \theta_i R_{||}(0) \cos(\eta_s - \eta_i) .$$

The above equations demonstrate the claim of Hagfors and other investigators who note that optics techniques applied to very rough surfaces models predict no depolarization for backscattering. The second and third optics models discussed previously clearly show that backscattering can come only from areas or facets on the rough surface which are oriented normal to the incidence direction. This also accounts for the appearance of the Fresnel reflection coefficients for normal incidence in the above equations.

Let us now give the results for average backscattering cross sections per unit area for the two probability density models proposed above, remembering that no depolarization is predicted.

a. Gaussian surface height probability function model

$$(56) \quad \sigma_{vv}^O = \sigma_{hh}^O = \sigma_{RL}^O = \sigma_{LR}^O = \sigma_{\eta_i \eta_i}^O$$

$$= \frac{\sec^4 \theta_i}{s^2} |R_{ii}(0)|^2 e^{-\frac{1}{s^2} \tan^2 \theta_i}$$

b. Exponential surface height probability function model

$$(57) \quad \sigma_{vv}^O = \sigma_{hh}^O = \sigma_{RL}^O = \sigma_{LR}^O = \sigma_{\eta_i \eta_i}^O$$

$$= \frac{3 \sec^4 \theta_i}{s^2} |R_{ii}(0)|^2 e^{-\frac{\sqrt{6}}{s} \tan \theta_i}$$

The first of the above equations has been given previously by Hagfors (1964) while the second is presented here for comparison. Curves illustrating the dependence of

$$\frac{\sigma^O}{|R_{ii}(0)|^2}$$

for the above two models upon angle of incidence,  $\theta_i$ , for various values of rms roughness slope,  $s$ , are presented in Fig. 6.

#### IV. COMPOSITE SURFACES

##### A. Explanation

Natural forces seldom create a "very rough" surface satisfying the restrictions of the preceding part. Rough surfaces arising in nature having roughness whose height is large compared to wavelength almost always also possess smaller scale roughnesses, such that the surface is not locally smooth. As examples, consider an area of mountainous terrain. The mountains and valleys alone comprise a roughness large

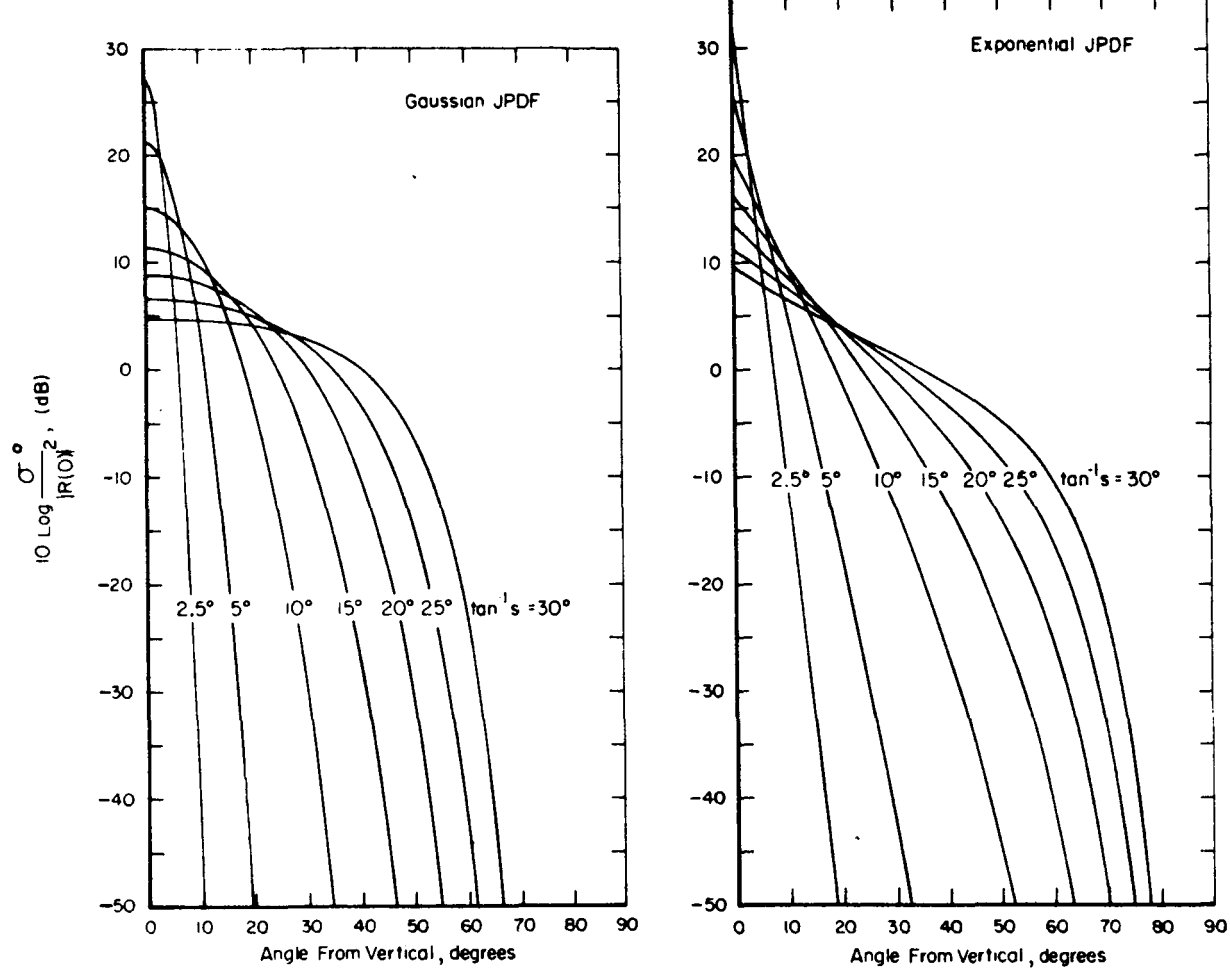


Fig. 6. Average incoherent backscattering cross section per unit area for very rough surface statistical model vs. incidence angle for any set of direct polarization states for two surface height JPDF (Joint Probability Density Function) models. Curves are normalized to the Fresnel reflection coefficients for normal incidence.

compared to wavelength for frequencies of VHF or higher. If no other smaller roughness were present, the analysis of the preceding section might be applied. However, the trees, rocks, and grassy fields also present constitute a roughness whose scale compared to wavelength may be small. Hence, the tangent plane restriction and optics approximation of the preceding part cannot be used without closer examination. The type of surface described above, characterized by both large and small scale roughnesses, will be called a "composite" surface.

Let us look again at the chief differences between the average incoherent backscattered power from the slightly rough surface and the very rough surface of the preceding parts. The slightly rough

surface, as shown in Fig. 2, produces a small backscattered field near normal incidence where  $\theta_i = 0$ , but this field may still be significant near grazing. As discussed previously the scattered power near grazing is directly related to the amount of surface roughness spectral strength at higher spatial frequencies; in particular, at and near frequency  $2k_0$  radians/meter. On the other hand, backscattering from very rough surfaces, as seen in Fig. 6, is much larger near normal incidence ( $\theta_i = 0$ ) but falls off rapidly away from normal.

The suggestion to be put forth here is that both the large scale and the small scale roughness contribute significantly to the scattering from natural, composite surfaces. Near the specular direction (i.e.,  $\theta_s = \theta_i$ ,  $\phi_s = 0$ ) scattering of the optics type, predicted by the very rough surface theories, predominates. At scattering angles considerably removed from this direction, however the smaller but persistent scattered power is due to the slight roughness present on top of the larger roughnesses.

In fact, to a first approximation, one may merely add the average incoherent scattering cross sections from the very rough surface model to that of the slightly rough surface model to obtain the total composite rough surface scattering cross section. An heuristic and physically intuitive proof of this statement will be given here, but for a more exact-albeit mathematically involved-proof, one can consult two recent Soviet articles of Semenov (1966) and Fuks (1966).

Consider first the very rough surface model of the preceding part. The surface to which it applies is smooth over regions of the order of a wavelength. The scattered power is incoherent and concentrated near the specular direction because the surface slopes are generally small and the probability is great that the local normal of any surface point is within a few degrees of the vertical. Now assume that a slight roughness "grows" on top of this very rough but locally smooth surface. This slight roughness does not greatly diminish the large specular scattering of the very rough surface, just as it did not diminish greatly the coherent scatter of the smooth plane over which it was imposed in Part 2. However, in directions considerably away from the specular (e.g., near grazing for backscatter), where the very rough surface model predicts very small scattered power, the slight roughness will produce an observable addition to the scattered power. Since the "very rough" portion of the surface has small surface slopes, the slight roughness can be approximated to a first order as being distributed over a smooth plane in computing the local angle of incidence. As seen in Figs. 2 and 3, small changes (say  $15^\circ$  or less) in the local angle of incidence,  $\theta_i$ , (due to local variations in the

underlying very rough surface slope) do not produce a marked change in backscattering cross section, so long as the spectral strength of the superimposed slight roughness is fairly constant out to approximately  $\frac{1}{2} k_0$  radians/meter. Hence the two average incoherent scattering cross sections may be simply added together, assuming the same incidence and scattering angles ( $\theta_i, \theta_s, \phi_s$ ) for both.

Actually, two averaging processes must take place. The slight roughness height variable and the large roughness height variable are averaged separately. This necessitates the additional restriction that the two different scales of roughness are statistically independent. Such is generally true when the two roughness scales are formed by different natural processes. For example, mountains and valleys are usually formed by an entirely different process than is the vegetation cover; hence the assumption of statistical independence between the distribution of these natural roughnesses, although not perfect, generally seems reasonable. Since the slight roughness and large roughness are statistically independent and each alone produces strictly an incoherent scattered power, we can perform the averaging of each separately and merely add the powers from each.

The above explanation is meant to be intuitive rather than rigorous. It is meant to provide physical insight rather than mathematical confusion. Mathematical proof is satisfying, however, and can be found in the above mentioned Soviet references. Generally the necessary restrictions are those given in the preceding two parts, along with the one mentioned in the preceding paragraphs. Neglected in this explanation is any possible roughness scale which is of intermediate size such that it does not fall entirely either in the very rough or the slightly rough category. Since most natural surfaces have a roughness component whose scale is of this order, the model here must be expected to give results which deviate somewhat from measured values. This deviation is expected for scattering geometries where the scattering cross section for the slight roughness alone is approximately equal to that for the large scale roughness. In general the predicted result will be too small, because any intermediate scale roughness will tend to add another scattered field component which will be significant in this region. Since no known theory is valid for intermediate scale roughness, this component cannot at present be taken into account quantitatively.

Western writers have attempted to treat composite rough surfaces. Beckmann (1965) and Hayre and Kaufman (1965) both treat this problem by a physical optics model. Their analysis does not truly apply to a slight roughness scale since it is based on an optics formulation.

This is evident from the results, which are functionally the same as for the very rough surface with a single large scale of roughness. The only difference is that the mean square slope,  $s^2$ , appearing in their results for the composite surface is written in terms of the sum of the mean square slopes of each of the roughness scales present. Their results are hence valid for all roughness scales down to those which can no longer be treated by their optics formulation (i.e., which no longer satisfy the restrictions of Part 3). They cannot apply to surfaces which include a true slight roughness component, however.

Radar experimentalists have in the past attempted to break the measured direct polarized backscatter cross section vs. incidence angle into two regions. The region near normal was called the specular region, and it was generally agreed to be predicted by the optics theories and results of Part 3. The "tail" of the echo, or that region near grazing was termed the "diffuse" region, and there has been no general agreement to date on a satisfactory explanation for its existence. Various investigators have attempted to fit empirical curves to this component; among the postulated are  $\cos \theta_i$ ,  $\cos^{3/2} \theta_i$ , and still others. Hagfors (1967) has suggested a model consisting of randomly oriented dipoles as accounting for this component. This is one of a large class of geometrical models with distributions of individual scatterers which lie outside the class of continuous surfaces we have been considering. (See Peake, 1967).

We wish to suggest here that this "diffuse" component is produced by the presence of slight and intermediate roughness scales and is predicted to a first order by the models of Part 2. We offer predicted curves based on the composite model presented here and compared them with measured results for backscatter.

The explanation for the depolarized backscattered component from composite surfaces is more complex, however. The optics theories predict no return. To the first order, the slightly rough model studied here also indicates no depolarized return for the vertical and horizontal states; depolarization for the circular states does appear, but is absent at normal incidence. The higher order terms, for example the second term as calculated by Valenzuela, do show depolarization, even for the vertical and horizontal states. As the roughness scale increases with respect to wavelength from slight to intermediate, these higher order terms containing depolarization effects become non-negligible. Since the perturbation theory breaks down as the smallness parameters approach unity, the contribution of the intermediate scale of roughness cannot be calculated. It is clear

from the trend of the higher order terms, however, that they will contribute significantly to both the polarized and depolarized components. It is our conclusions, therefore, that depolarization for backscatter is produced by two mechanisms: (a) the slight and intermediate roughness scales just discussed, and (b) multiple reflections from suitably oriented surface elements of the large scale roughness for surfaces where the reflection coefficients are polarization dependent.

To illustrate the predictions of the composite surface model, Figs. 7 provide curves for horizontal and vertical polarization states for a variety of dielectric constants and model parameters. They are made by simply adding the backscattering cross sections for the slightly rough model to those of the very rough model. More curves of this type can be found in Radar Cross Section Handbook (1968). Figure 8 shows the measured cross section of the sea surface on a calm day made for the vertical and horizontal states; these are also taken from the above reference. The similarity is convincing. Note that none of these curves represents a depolarized component; the received polarization state is in each case the same as the transmitted.

For the circular polarization states, one can construct the same type of curves, which results are sort of a superposition of the curves of Fig. 3 with those of Fig. 6. They are not shown here but may be found in the preceding reference. It should be noted, however, that the curve representing the depolarized component is not actually a composite, because the very rough surface contribution to backscattering in this case zero: only the slight roughness produces depolarization. One set of curves for circular polarization is compared to a measured set from the lunar surface at  $\lambda_0 = 68$  cm in Fig. 9. Measured results were taken from the work of Evans and Pettingill (1963), and were normalized with respect to the measured cross section of the entire moon at this frequency. The set of model curves was selected on the basis of best fit. From the model for this best fit, the following parameters for the lunar surface are indicated:  $\epsilon_r$  = dielectric constant = 2.9,  $\tan^{-1} s_1$  = large scale roughness slope =  $12^\circ$ ,  $h_2$  = rms slight roughness height = 2 cm,  $\tan^{-1} s_2$  = slight roughness slope =  $27^\circ$ . The comparison of the measured and predicted depolarized components shows lack of agreement near normal incidence. This is expected for the following reasons: (i) Hagfors (1967) reports that the ability to isolate one measured circular state from the other was probably not greater than 18 dB. Hence near normal where the polarized component is very strong, most of the "measured" depolarized component may actually be the polarized component. (ii) The intermediate scale roughness, which cannot be accounted for by the theory, most likely produces depolarization. As mentioned previously, this effect is likely to appear further away from grazing, i.e., near normal incidence.

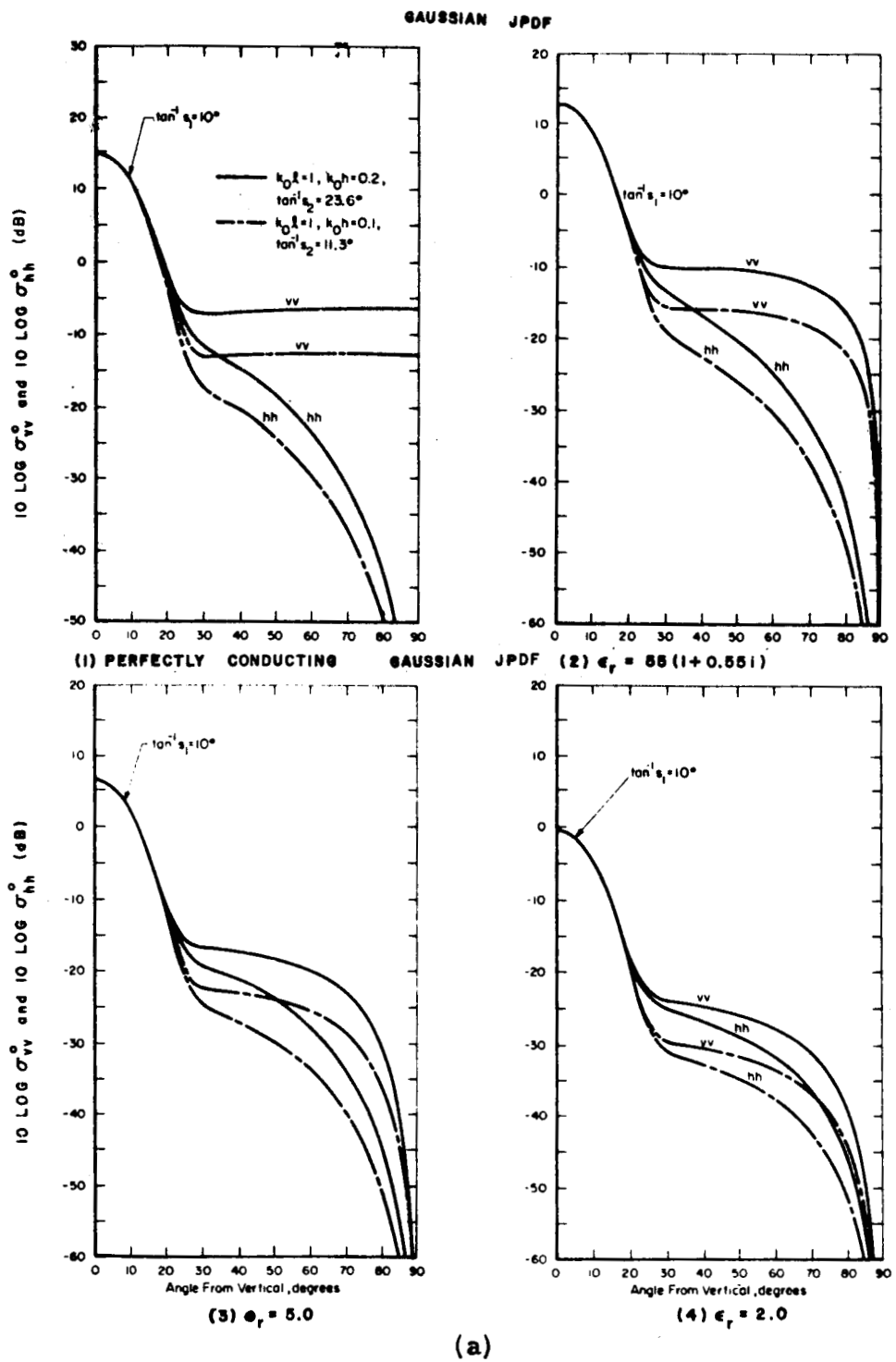


Fig. 7a. Average backscattering cross section per unit area for composite rough surface model vs. incidence angle for various large scale roughness parameters,  $s_1$ , and small scale roughness parameters,  $k_0 l$  and  $k_0 h$  (or  $s_2$ ). Linear polarization states. (a) Gaussian large scale roughness height probability density model.

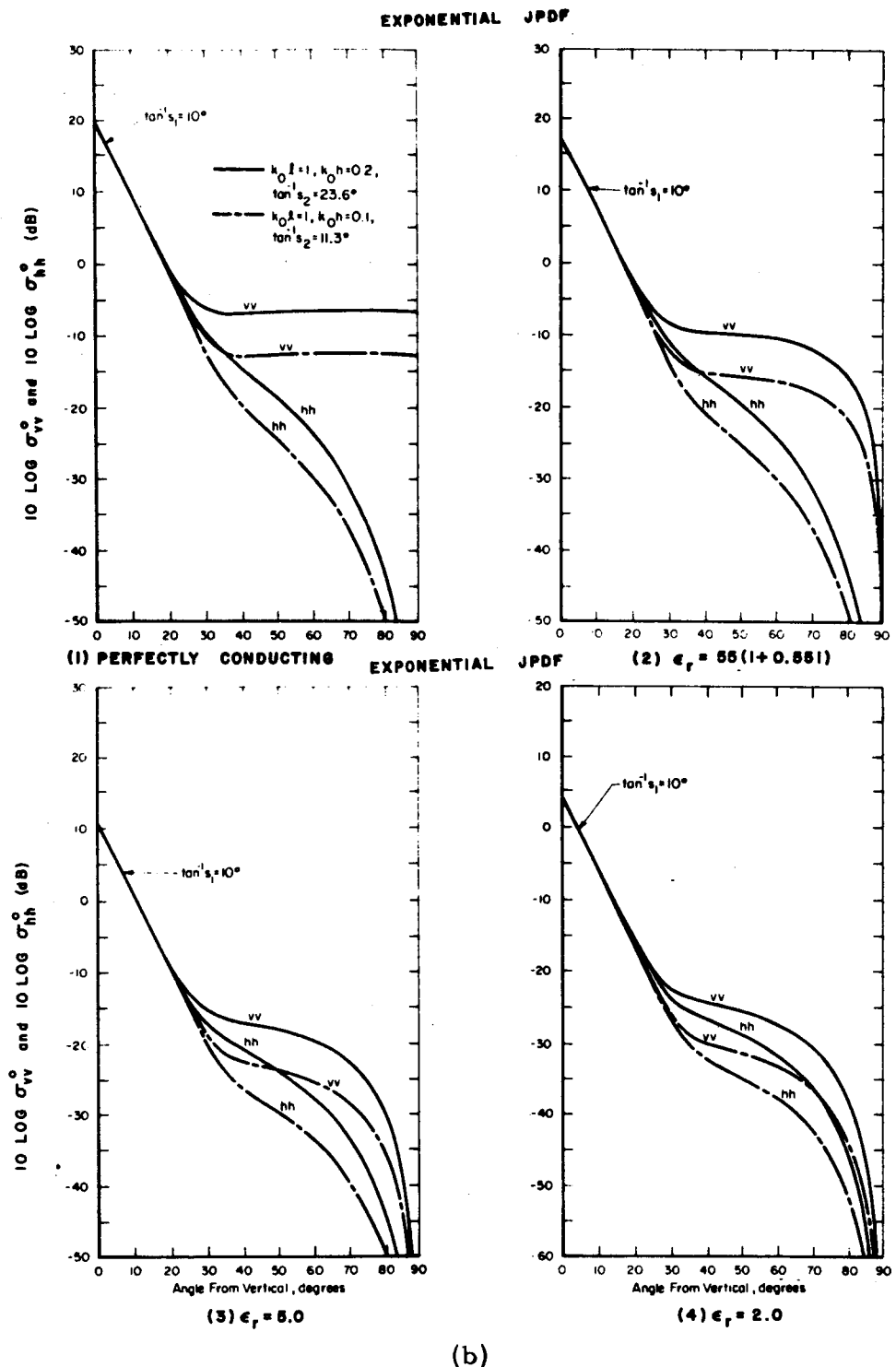
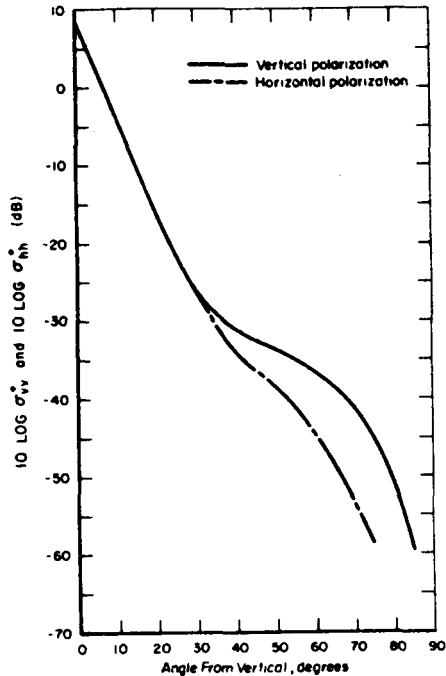


Fig. 7b. Exponential large scale roughness height probability density model.

Fig. 8. Measured average back-scattering cross section per unit area from relatively calm sea surface at X-band vs. incidence angle for vertical and horizontal polarization states.

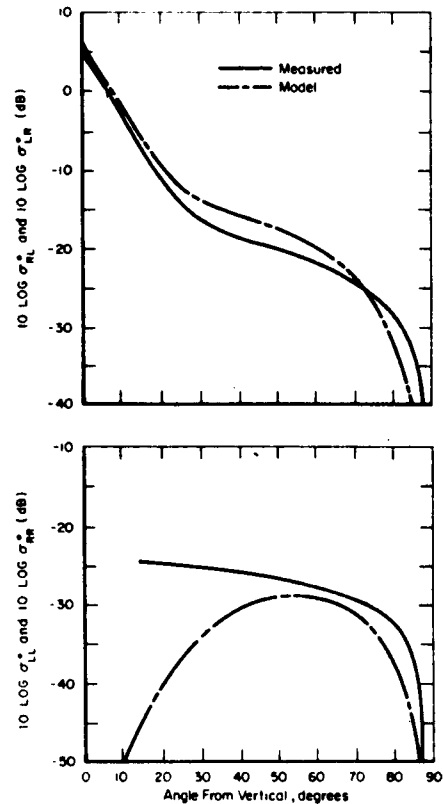


## V. ROUGH SPHERICAL SURFACE - BACKSCATTERING CROSS SECTION

### A. Introduction

The past sections have derived the average incoherent scattering cross section per unit area for a rough planar surface, i.e., a surface whose mean value is a plane. In this section we will extend these results to a rough spherical surface. Such a situation is representative, for example, of a planetary surface, or of many spherical satellites of the Echo I and II variety whose surfaces are somewhat rough. In defining the average backscattering cross section of a rough spherical surface, we understand that the entire sphere is immersed simultaneously in the illuminating field. This may not be the case, for example, in many of the planetary radar studies where a short pulse sweeps past the planet, illuminating only an annular area at a time.

Fig. 9. Measured average back-scattering cross section per unit area from lunar surface at UHF ( $\lambda = 68$  cm) vs. incidence angle with circular polarization states. Dashed curves represent composite rough surface model, presented for comparison. Upper curves represent opposite sense polarization states, lower curves - same sense.



The results of the preceding sections can be used to obtain the incoherent backscattering cross sections for both very rough and slightly rough spheres. Furthermore, for the slightly rough sphere, there will be a significant coherent component due predominantly to reflection from the front cap, and this will also be estimated.

It is assumed that the radius of the sphere  $A_R$ , is much larger than both the wavelength,  $\lambda$ , and roughness height correlation length,  $\ell$ . It is further assumed that the sphere is large enough and its material lossy enough that waves entering the sphere do not further contribute to the scattering. In addition, all of the restrictions of the preceding sections apply.

### B. Coherent Backscattering Cross Section

It was mentioned in Part I that the coherent scatter from any slightly rough surface is highly dependent upon the shape of the illuminated surface in the absence of roughness. The presence of roughness is taken into account by modifying the Fresnel reflection coefficients at the surface, as in Eq. (1). The reflected complex fields in this case, being coherent and having a non-zero average value, can be treated just as they would be from a smooth surface; stationary phase analysis predicts that nearly the entire coherent backscattered field in this case comes from the front specular cap. Hence the average coherent backscatter cross section from a slightly rough spherical surface becomes

$$(58) \quad \sigma = \pi A^2 R |R(0)|^2 e^{-4k_0^2 h^2},$$

where

$$(59) \quad R(0) = \frac{\sqrt{\epsilon_r} - \sqrt{\mu_r}}{\sqrt{\epsilon_r} + \sqrt{\mu_r}}$$

is the Fresnel reflection coefficient for a smooth planar surface at normal incidence. The effect of surface roughness near the specular cap is accounted for by the exponential factor involving the mean square roughness height,  $h^2$ . The above result, having come from the use of the slightly rough surface reflection coefficients of Eq. (1) is valid for surfaces having a Gaussian distributed roughness height. One sees that as rms roughness height increases to where  $k_0 h > 1$ , the coherent cross section decreases rapidly.

The polarization states of the scattered coherent field above is the same as it would be in the absence of roughness, i.e., there is no depolarization predicted.

### C. Average Incoherent Backscattering Cross Section - Slightly Rough Surface

The average incoherent backscattering cross sections for a slightly rough spherical surface are computed from the preceding results for a rough planar surface. Use is made of the property of

incoherent power which permits one to merely add the power backscattered from one portion of the surface to that from another portion, rather than adding the complex scattered fields themselves. Recall that  $\sigma_{\gamma\delta}^0$  is the average incoherent backscattered power per unit mean surface area (where  $\theta_s = \theta_i$  and  $\phi_s = \pi$  in the equations for  $\sigma_{\gamma\delta}^0$ ). Then the backscattering cross section for a mean spherical area element  $dA = A_R^2 \sin \theta_i d\theta_i d\phi$  is the product of  $dA$  and  $\sigma_{\gamma\delta}^0$ . The total average backscattering cross section is then determined by integrating over the entire illuminated hemisphere, i.e.,

$$(60) \quad \sigma_{\gamma\delta} = A_R^2 2\pi \int_0^{\pi/2} \sigma_{\gamma\delta}^0 \sin \theta_i d\theta_i$$

where the integration over  $\phi$  has been performed since the integrand is not a function of  $\phi$ . The spherical coordinate system has been chosen here so that the polar axis coincides with the direction of propagation, making the polar angle  $\theta_i$  also the angle of incidence upon the spherical surface.

For the aligned and crossed incident and received linear polarization states, the expressions which must be substituted into the above equation for  $\sigma_{\gamma\delta}^0$  are those given in Eqs. (19) and (31). The integration over  $\phi$  corresponds to the integration over  $\eta_i$  which was already performed in deriving Eqs. (31). The integration over  $\theta_i$  demanded in the above equation can only be performed numerically. The resulting cross sections normalized as

$$\frac{\sigma}{\pi A_R^2 k_o^2 h^2},$$

are plotted in Fig. 10 vs  $k_o \ell$  for various values of surface dielectric constant. This is done for both the aligned and crossed linear states (representing the polarized and depolarized return) and for the Gaussian and exponential surface height correlation coefficient models. Note that as  $k_o \ell$  becomes larger the depolarized component becomes smaller. This is expected, since larger  $k_o \ell$  corresponds to a smoother surface. Note that the terminology vertical and horizontal states have no significance when referred to a sphere.

For the circular polarization states, the appropriate curves are found in Radar Cross Section Handbook (1968). They are nearly identical with those for the linear states in the cases of the polarized components;

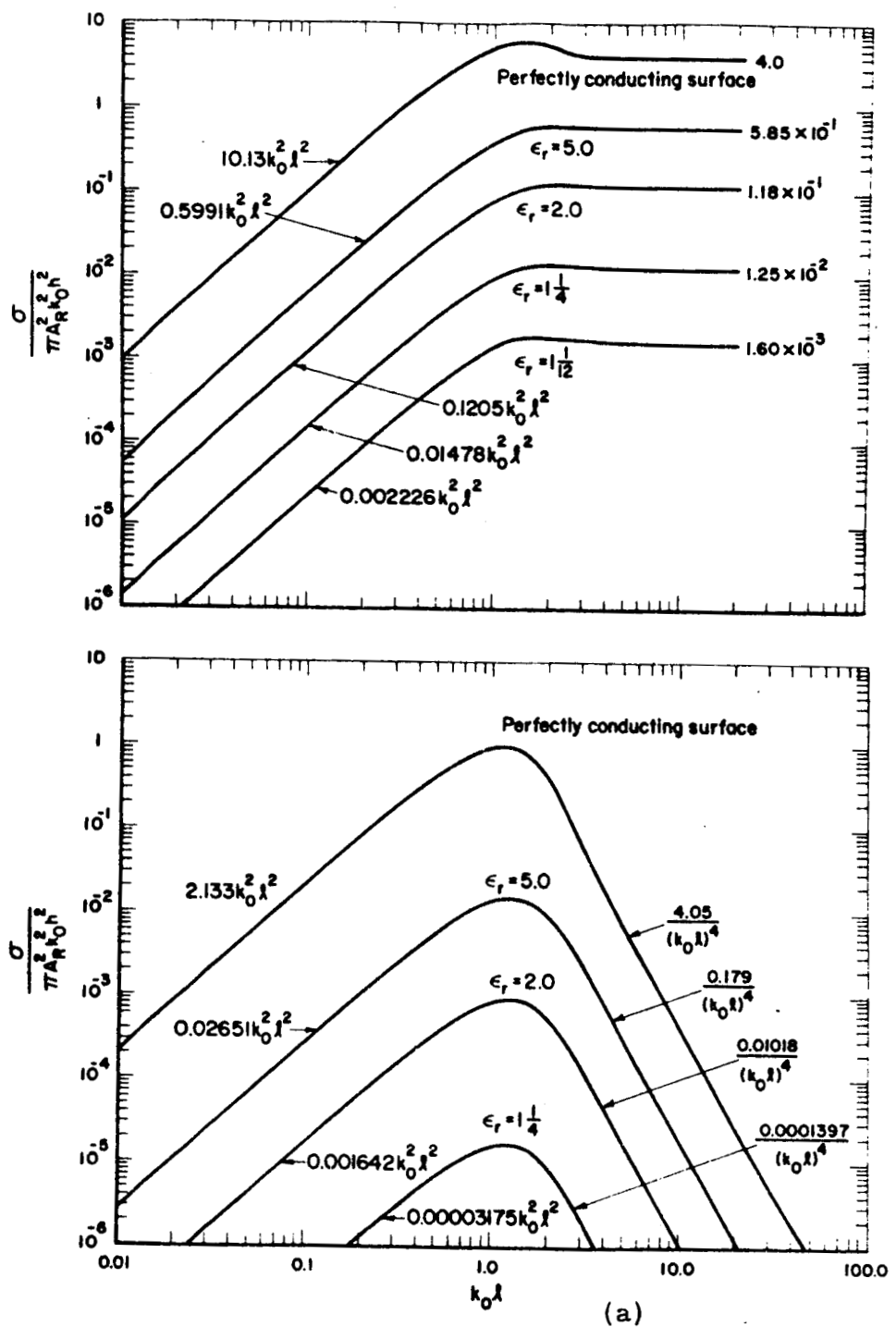


Fig. 10a. Average incoherent backscattering cross section for slightly rough spherical surface of mean radians  $A_r$  as a function of  $k_0 l$ . Cross section is normalized to  $\pi A_r k_0^2 h^2$ . Linear polarization states, upper curves represent same sense received as transmitted, lower curves - perpendicular sense received. (a) Gaussian height correlation coefficient model.

PAGES 55 AND 56 ARE MISSING FROM THE  
ORIGINAL DOCUMENT.

and plotted as a function of the arctangent of the rms roughness slope,  $s$  (i.e.,  $s = (2h/\lambda)$ ). This function is sometimes referred to as the roughness gain of the sphere. The two curves represent the two probability density function models discussed in Part III. Noteworthy, however, is the fact that as roughness increases, the backscattering cross sections become larger than that for a smooth sphere.

It is seen that as the surface becomes smooth (i.e.,  $s \rightarrow 0$ ), the backscattering cross sections do indeed approach those for a smooth sphere i.e.,  $\sigma = \pi A_R^2 |R(0)|^2$ . The figures are of questionable validity for  $\tan^{-1} s > 45^\circ$  because of the restrictions under which they were derived. For typical surface slopes much beyond  $45^\circ$ , shadowing and multiple scattering are no longer negligible. In the roughness slope region less than  $45^\circ$  the increase in scattering cross section from the smooth sphere limit is not appreciable. Hence an important conclusion for planetary surface backscatter can be drawn:

Large scale surface roughness for all practical purposes can be neglected and the total average backscattering cross section can be taken to be that for a smooth sphere,  

$$\sigma = \pi A_R^2 |R(0)|^2$$

Consequently, knowing the approximate radius of the body,  $A_R$ , an estimate of the surface dielectric constant can be made from a measurement of  $\sigma / \pi A_R^2$ ; for the moon for the range  $5 \text{ cm} < \lambda < 100 \text{ cm}$  one obtains approximately  $|R(0)|^2 = 0.07$ . Such a value of  $|R(0)|^2$  implies an effective dielectric constant of  $\epsilon_r = 2.9$ .

#### E. Average Incoherent Backscattering Cross Section - Composite Surface

As mentioned previously, most natural surfaces consists of roughness scales both larger and smaller than wavelength. As shown in Part IV, one can add the incoherent backscattering cross sections of the preceding sections (presented in Figs. 10 and 11) to obtain the effective total backscattering cross section of the composite surface. However, the backscattering cross section for the slight roughness, being proportional to  $k_0^2 h^2$ , is small, since this parameter is restricted to small values. Hence only the large scale roughness contributes significantly to the backscattered power for the polarized received component. On the other hand, since only the slight roughness scale is

responsible for the depolarized component, according to these models, it alone may be the best available estimate for this component.

## VI. SUMMARY

We have attempted to set forth what we believe to be the soundest analyses and solutions for rough surface scattering that are presently available. In addition, we have enumerated the restrictions under which the results are valid. Finally, we have interpreted physically the scattering mechanism behind the mathematics.

A slightly rough surface produces strong coherent reflection near the specular direction and a weaker incoherent scatter in other directions. An estimate of the coherent reflection can be computed just as it is for a smooth surface, making use of the reflection coefficients of Eq. (1); the resulting scattering pattern is strongly dependent upon the shape of the illuminated area and exhibits a lobe structure. The incoherent scatter was dealt with in more detail by a perturbation technique rather than the less valid tangent plane approximation. It was shown that incoherent scattered power from a slightly rough surface of either homogeneous material or a perfectly reflecting interface is directly proportional to the roughness spectral densities. The highest roughness spectral components which can affect the process are those near  $2k_0$  radians/meters. These are responsible for backscatter near grazing incidence. Lower roughness spectral frequencies produce scattering closer to the specular direction. For the important case of backscatter, significant differences exist between the cross sections near grazing for the vertical and horizontal states; vertical transmit and receive antennas produce considerably more return than horizontal, a fact which is confirmed experimentally. The solutions, including only the lowest order perturbation terms, exhibit no depolarization for the vertical and horizontal states. From the solutions for vertical and horizontal polarizations, results for the circular states and arbitrarily oriented linear transmit and receive states are given.

The only presently satisfactory methods for treating very rough surfaces are optics techniques; basic to all of these is the tangent plane restriction. A physical interpretation of the scattering process can be based upon any of the well known optics principles. Three techniques (i.e., physical optics, ray optics, and the specular point or stationary phase principle) all give identically the same result. Scattering in a given direction takes place as a result of surface facets so oriented that they specularly reflect. As would be expected from such a theory, backscattered power is not depolarized. Two probability density function

models are chosen for the surface height; for both, the curves of back-scattered power show strong return near normal incidence (the specular direction) which falls off rapidly as grazing is approached. The only surface height correlation coefficient which can be employed with these techniques is one which is parabolic in behavior for small surface separations.

Natural surfaces which are very rough in height compared to wavelength almost always have smaller scale roughnesses superimposed; these are called composite surfaces. As one might expect, the slightly rough and very rough surface scattering theories together account in part for the return. In the case of backscatter near vertical, for instance, the return is dominated by the very rough surface predicted scatter. Near grazing, however, the smaller roughness scales usually account for the return. Curves for backscattering cross section are shown for these composite models at various set of parameters for the vertical and horizontal polarization states. These are compared with measured data from the lunar and sea surface.

Backscatter from roughened spherical surfaces, which has application to planetary probing and passive satellite communications, is treated in Part V. The coherent and incoherent average backscattering cross sections are obtained, the latter in graphical form resulting from a numerical integration. Very rough spherical surfaces are also treated, and it is shown that the roughness in this case has little effect on the backscatter relative to that of a smooth sphere; in reality, the roughness slightly increases the cross section.

## REFERENCES

Barrick, D., (1965), "A More Exact Theory of Backscattering from Statistically Rough Surfaces," Report 1388-18, 31 August 1965, Antenna Laboratory, The Ohio State University Research Foundation; prepared under Grant NSG-213-61, National Aeronautics and Space Administration, Washington, D.C.

Barrick, D., (1968), "On the Permissible Form for the Surface Height Correlation Coefficient in Scattering from Very Rough Surfaces," correspondence, to be published.

Barrick, D., (1968), "Rough Surface Scattering Based on the Specular Point Theory," to be published.

Beckmann, P. and A. Spizzichino, (1963), The Scattering of Electromagnetic Waves from Rough Surfaces, MacMillan Company.

Beckmann, P., (1965), "Scattering by Composite Rough Surfaces," Proceedings of the IEEE, 53, No. 8, p. 1012.

Beckmann, P., (1965), "Shadowing of Random Rough Surfaces," IEEE Transactions on Antennas and Propagation, AP-13, p. 384.

Brockelman, R., and Hagfors, T., (1966), "Note on the Effect of Shadowing on the Backscattering of Waves from a Random Rough Surface," IEEE Transactions on Antennas and Propagation, AP-14, p. 621.

Cosgriff, R., W. Peake, and R. Taylor, (1960), Terrain Scattering Properties for Sensor System Design, (Terrain Handbook II), The Ohio State University, Engineering Experiment Station Bulletin No. 181.

Daniels, F., (1961), "A Theory of Radar Reflection from the Moon and Planets," Journal of Geophysical Research, 66, p. 1781.

Davenport, W. and W. Root, (1958), An Introduction to the Theory of Random Signals and Noise, McGraw-Hill Book Company, New York.

Davies, H., (1954), "The Reflection of Electromagnetic Waves from a Rough Surface," Proceedings of the IEE (Great Britain), 101, Part IV, p. 209.

Evans, J., and G. Pettengill, (1963), "The Scattering Behavior of the Moon at Wavelengths of 36, 68, and 784 Centimeters," *Journal of Geophysical Research*, 68, p. 423.

Fuks, I., (1966), "Contribution to the Theory of Radio Wave Scattering on the Perturbed Sea Surface," *Izvestia Vyshikh Uchebnikh Zavedeniy, Radiofizika*, 5, p. 876, (English Translation).

Fung, A., (1964), "Theory of Radar Scatter from Rough Surfaces, Bistatic and Monostatic, with Application to Lunar Radar Return," *Journal of Geophysical Research*, 69, p. 1063.

Fung, S., Moore, R., and Parkins, B., (1965), "Notes on Back-scattering and Depolarization by Gently Undulating Surfaces," *Journal of Geophysical Research*, Vol. 70, No. 6, p. 1559.

Hagfors, T., (1960), "Some Properties of Radio Waves Reflected from the Moon and Their Relationship to the Lunar Surface," Report No. 8, Radioscience Laboratory of Stanford Electronics Laboratories.

Hagfors, T., (1964), "Backscattering from an Undulating Surface with Applications to Radar Returns from the Moon," *Journal of Geophysical Research*, 69, p. 3779.

Hagfors, T., (1966), "Relationship of Geometric Optics and Auto-correlation Approaches to the Analysis of Lunar and Planetary Radar," *Journal of Geophysical Research*, Vol. 71, No. 2, p. 379.

Hagfors, T., (1967), "A Study of the Depolarization of Lunar Radar Echoes," *Radio Science*, Vol. 2, No. 5, p. 445.

Hayre, H., (1961), "Theoretical Scattering Coefficient for Near Vertical Incidence from Contour Maps," *Journal of Research, National Bureau of Standards, Section D - Radio Propagation*, 65D, No. 5, p. 427.

Hayre, H., and D. Kaufman, (1965), "Plane-Wave Scattering from a Rough Surface with Correlated Large- and Small-Scale Orders of Roughness," *Journal of Acoustical Society of America*, 38, No. 4, p. 599.

Hughes, V., (1962), "Diffraction Theory Applied to Radio Wave Scattering from the Lunar Surface," *Proceedings of Physical Society*, 68, Vol. 80, Part 5, p. 1117.

Isakovich, M., (1952), "The Scattering of Waves from a Statistically Rough Surface," *Zhurnal Eksperimental'noi Teoreticheskoi Fiziki* (USSR), 23, (English translation by Morris Friedman).

Kivelson, M., and Moszkowski, S., (1965), "Reflection of Electromagnetic Waves from a Rough Surface," *Journal of Applied Physics*, Vol. 36, p. 3609.

Kodis, R., (1966), "A Note on the Theory of Scattering from an Irregular Surface," *IEEE Transactions on Antennas and Propagation*, AP-14, No. 1, p. 77.

Middleton, D., (1960), "An Introduction to Statistical Communication Theory," McGraw Hill Book Company, New York.

Muhleman, D., (1964), "Radar Scattering from Venus and the Moon," *The Astronomical Journal*, 69, No. 1, p. 34.

Peake, W., (1959), "The Interaction of Electromagnetic Waves with Some Natural Surfaces," Ph.D. Dissertation, The Ohio State University. Also appears as Report 898-2, 30 May 1959, Antenna Laboratory, The Ohio State University Research Foundation; prepared under Contract AF 33(616)-6158, Wright Air Development Center, Wright-Patterson Air Force Base, Ohio; also "Theory of Radar Return from Terrain," IRE Convention Record, Vol. 7, p. 27.

Peake, W.H., (1967), "Scattering from Rough Surfaces Such as Terrain." Chapter in Antennas and Scattering Theory, to be published by Boston Technical Publishing Co.

Rayleigh, (1945), The Theory of Sound, Vols. I and II, Dover Publishers.

Rice, S., (1944, 1945), "Mathematical Analysis of Random Noise," Parts I and II, *Bell System Technical Journal*, 23, p. 282, and Parts III and IV, 24, p. 46.

Rice, S., (1963), "Reflection of Electromagnetic Waves by Slightly Rough Surfaces," in The Theory of Electromagnetic Waves, edited by M. Kline, Interscience Publishers, also Dover.

Ruck, G.; Barrick, D.; Stuart, W., and Krichbaum, C., Radar Cross Section Handbook, Chapter 9, to be published by Plenum Press.

Semenov, B., (1965), "Scattering of Electromagnetic Waves from Restricted Portions of Rough Surfaces with Finite Conductivity," *Radiotekhnika i Elektronika* (USSR), 10, 1. 1952 (English Translation).

Semenov, B., (1966), "An Approximate Calculation of Scattering of Electromagnetic Waves from a Slightly Rough Surface," *Redioteknika i Elektronika (USSR)*, 11, p. 1351 (English Translation).

Stogryn, A., (1967), "Electromagnetic Scattering from Rough, Finitely Conducting Surfaces," *Radio Science*, Vol. 2, No. 4, p. 415.

Twersky, V., (1957), "On Multiple Scattering of Waves by Rough Surfaces," *IRE Transactions on Antennas and Propagation*, 5, p. 81.

Valenzuela, G., (1967), "Depolarization of EM Waves by Slightly Rough Surfaces," *IEEE Transactions on Antennas and Propagation*, AP-15, No. 4, p. 552.

Wagner, R., (1967), "Shadowing of Randomly Rough Surfaces," *Journal of the Acoustical Society of America*, Vol. 41, No. 1, p. 138.